The laminin-binding integrins regulate nuclear factor kappaB-dependent epithelial cell polarity and inflammation

Eugenia M. Yazlovitskaya, Erin Plosa, Fabian Bock, Olga M. Viquez, Glenda Mernaugh, Leslie S. Gewin, Adele de Arcangelis, Elisabeth Georges-Labouesse, Arnoud Sonnenberg, Timothy S. Blackwell, et al.

© 2021. Published by The Company of Biologists Ltd | Journal of Cell Science (2021) 134, jcs259161. doi:10.1242/jcs.259161

RESEARCH ARTICLE

The laminin-binding integrins regulate nuclear factor κB-dependent epithelial cell polarity and inflammation

Eugenia M. Yazlovitskaya[1], Erin Plosa[2], Fabian Bock[1], Olga M. Viquez[1], Glenda Mernaugh[1], Leslie S. Gewin[1,3,4], Adele De Arcangelis[5], Elisabeth Georges-Labouesse[5,*], Arnoud Sonnenberg[6], Timothy S. Blackwell[3,4,7], Ambra Pozzi[1,3] and Roy Zent[1,3,4,‡]

ABSTRACT

The main laminin-binding integrins α3β1, α6β1 and α6β4 are co-expressed in the developing kidney collecting duct system. We previously showed that deleting the integrin α3 or α6 subunit in the ureteric bud, which gives rise to the kidney collecting system, caused either a mild or no branching morphogenesis phenotype, respectively. To determine whether these two integrin subunits cooperate in kidney collecting duct development, we deleted α3 and α6 in the developing ureteric bud. The collecting system of the double knockout phenocopied the α3 integrin conditional knockout. However, with age, the mice developed severe inflammation and fibrosis around the collecting ducts, resulting in kidney failure. Integrin α3α6-null collecting duct epithelial cells showed increased secretion of pro-inflammatory cytokines and displayed mesenchymal characteristics, causing loss of barrier function. These features resulted from increased nuclear factor kappa-B (NF-κB) activity, which regulated the Snail and Slug (also known as Snai1 and Snai2, respectively) transcription factors and their downstream targets. These data suggest that laminin-binding integrins play a key role in the maintenance of kidney tubule epithelial cell polarity and decrease pro-inflammatory cytokine secretion by regulating NF-κB-dependent signaling.

KEY WORDS: Inflammation, Cytokines, Fibrosis, Epithelial-to-mesenchymal transition

INTRODUCTION

The kidney collecting system develops from the ureteric bud by undergoing iterative branching events after interacting with the metanephric mesenchyme (MM), which gives rise to the nephrons (Carroll and Das, 2013). This process requires growth factor-mediated cell signaling and integrin-dependent cell-extracellular matrix (ECM) interactions (Mathew et al., 2012).

Integrins, the principal ECM-binding receptors, consist of non-covalently bound α and β transmembrane subunits. The 24 integrins found in mammals are made up from 18 α and eight β subunits that combine in a restricted manner to form specific αβ heterodimers with different ligand binding properties (Pozzi and Zent, 2003, 2011). Integrins link the ECM with the intracellular actin cytoskeleton and function as cell signaling molecules. Traditionally, they are thought to promote cell adhesion, migration and proliferation; however, more recently, integrins were shown to regulate epithelial cell inflammation (De Arcangelis et al., 2017; Niculescu et al., 2011; Plosa et al., 2020, 2014) and terminal differentiation (Vijayakumar et al., 2008). Integrins α3β1, α6β1 and α6β4 act as the major receptors for laminins (Yamada and Sekiguchi, 2015). The principal laminins found in the developing and adult collecting system of the kidneys are laminin-111, -511, -521 and -332 (Yazlovitskaya et al., 2015). Preferred ligands for integrin α3β1 include laminin-511, -521 and -332. Integrin α6β1 is the most promiscuous laminin receptor and binds laminin-111, -511, -521 and -322, and integrin α6β4 preferentially binds to laminin-332; however, it also interacts with laminin-511 and -521 (Delwel et al., 1994; Niessen et al., 1994; Viquez et al., 2017; Yazlovitskaya et al., 2015; Yazlovitskaya et al., 2019).

The contribution of the integrins in the developing kidney collecting system is incompletely understood. Kidney collecting duct epithelial cells grow on a basement membrane that consists of both collagen IV and laminins. Deletion of the integrin β1 subunit, which results in loss of expression of all αβ1 integrin heterodimers in the developing ureteric bud, resulted in a severe branching morphogenesis phenotype due to decreased epithelial cell adhesion, migration and proliferation (Zhang et al., 2009). Identification of the specific α subunits that regulate this process is inconclusive. The collagen binding integrins α1β1 and α2β1 do not contribute to kidney collecting system development (Mathew et al., 2012). Surprisingly, deletion of the integrin α3 subunit in the kidney collecting system only caused a mild branching morphogenesis phenotype (Kreidberg et al., 1996; Liu et al., 2009; Yazlovitskaya et al., 2015), and deletion of the α6 subunit (resulting in no expression of α6β1 and α6β4) did not result in any branching morphogenesis phenotype (Viquez et al., 2017).

To determine whether integrin α3 and the α6 integrins cooperate in kidney collecting duct development, we deleted both the α3 and α6 integrin subunits in the developing mouse ureteric bud. Surprisingly, the mice showed a mild renal developmental phenotype, but they all died by 14 months of age from severe inflammation around the collecting ducts and tubulointerstitial fibrosis mediated by epithelial cells that have acquired a more mesenchymal phenotype. We used α3/α6-null (Itgα3$^{-/-}$α6$^{-/-}$) collecting duct cells to show that the

[1]Division of Nephrology and Hypertension, Department of Medicine, Vanderbilt University Medical Center, Nashville, TN 37232, USA. [2]Division of Neonatology, Department of Pediatrics, Vanderbilt University Medical Center, Nashville, TN 37232, USA. [3]Veterans Affairs Hospital, Nashville, TN 37232, USA. [4]Department of Cell and Developmental Biology, Vanderbilt University School of Medicine, Nashville, TN 37232, USA. [5]Department of Development and Stem Cells, Institut de Génétique et de Biologie Moléculaire et Cellulaire, CNRS UMR7104, INSERM U964/ULP, F-67404 Illkirch, France. [6]Division of Cell Biology, Netherlands Cancer Institute, 1066 CX Amsterdam, Netherlands. [7]Division of Pulmonary and Critical Care Medicine, Department of Medicine, Vanderbilt University Medical Center, Nashville, TN 37232, USA.
*Deceased

‡Author for correspondence (roy.zent@vumc.org)

E.P., 0000-0001-7165-1722; F.B., 0000-0002-0788-2945; O.M.V., 0000-0002-3670-6924; G.M., 0000-0003-0463-9509; L.S.G., 0000-0002-6146-1092; A.D.A., 0000-0003-1114-8441; T.S.B., 0000-0002-0337-7052; R.Z., 0000-0003-2983-8133

Handling Editor: Kathleen Green
Received 18 July 2021; Accepted 18 November 2021

Journal of Cell Science (2021) 134, jcs259161. doi:10.1242/jcs.259161

inflammatory and mesenchymal phenotypes were mediated by increased activation of the nuclear factor kappa-B (NF-κB) transcription factor pathway that induced pro-inflammatory cytokine production and cadherin switching. Thus, laminin-binding integrins play a key homeostatic role in kidney collecting duct cells by suppressing NF-κB-dependent signaling.

RESULTS

Hoxb7cre:Itgα3$^{flox/flox}$ kidneys have excessive inflammation and fibrosis

We previously deleted Itgα3 in the developing ureteric bud, which resulted in a mild branching morphogenesis defect that became evident at embryonic day (E)15.5 and persisted into adulthood (Yazlovitskaya et al., 2015). By contrast, deleting Itgα6 in the ureteric bud did not cause a developmental phenotype (Viquez et al., 2017). In this study, we deleted the integrin α3 and α6 subunits in the developing ureteric bud by crossing the Itgα3/6$^{flox/flox}$ (also referred to here as α3$^{f/f}$α6$^{f/f}$) mice with Hoxb7Cre mice. This strategy successfully deleted these genes, resulting in decreased expression of the integrin α3 and α6 subunits in the pelvis of the kidney of 1-week-old mice, as assessed by immunoblotting. There was also a slight decrease in β1 integrin subunit expression; however, it was still robustly expressed (Fig. 1A). We confirmed β1 integrin expression in the aquaporin 2-expressing collecting ducts by immunofluorescence (Fig. 1B,C). When we performed a morphological examination of the kidneys from E15.5 and newborn mice, there appeared to be a mild branching morphogenesis defect in the Hoxb7cre:Itgα3/6$^{flox/flox}$ mice (Fig. 1D-G). We verified there were significantly less aquaporin 2-expressing collecting ducts in the kidneys of newborn Hoxb7cre:Itgα3/6$^{flox/flox}$ mice by immunostaining followed by quantification. (Fig. 1H-N). Thus, a mild branching morphogenesis defect was confirmed in Hoxb7cre:Itgα3/6$^{flox/flox}$ mice at birth.

We next assessed the long-term consequences of this mild branching defect on Hoxb7cre:Itgα3/6$^{flox/flox}$ mice. The mice lost weight as they aged, started to die at about 200 days old and were all dead or euthanized by 480 days (Fig. 2A). Their median survival

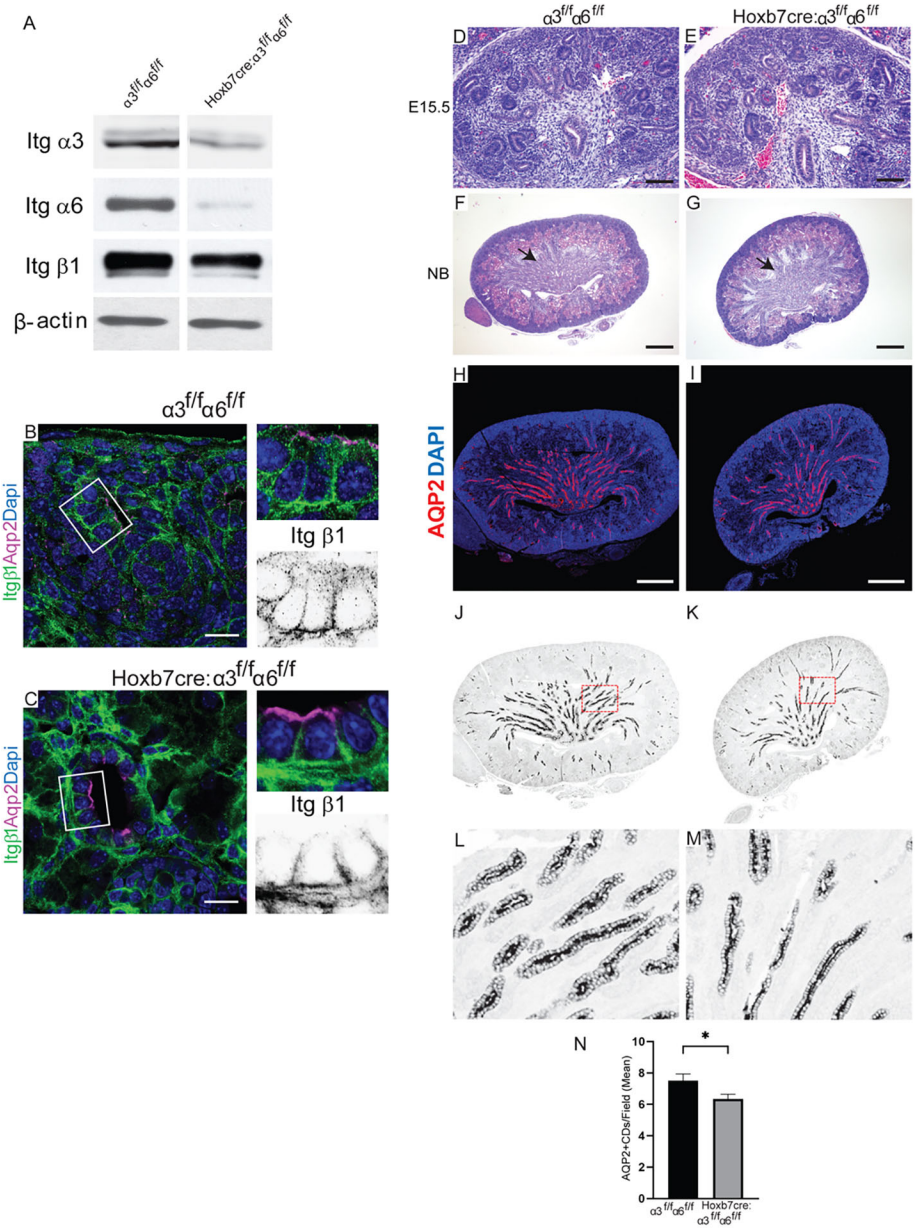

Fig. 1. Deletion of integrin α3 and α6 subunits in the ureteric bud results in a subtle branching morphogenesis defect. (A) Lysates of papillae (20 µg total protein/lane) from 3-day-old α3$^{f/f}$α6$^{f/f}$ and Hoxb7cre:α3$^{f/f}$α6$^{f/f}$ mice were analyzed by western blot for levels of integrin subunits α3, α6 and β1; β-actin was used as a loading control. (B,C) β1 integrin immunostaining (Itgβ1, green) and DAPI staining (blue) were performed on 3-day-old paraffin kidney sections, and the ureteric bud was labeled with aquaporin 2 (Aqp2; magenta), with magnified areas highlighted by white boxes. The black and white panels are grayscale conversions of the Aqp2 channel using the lookup table (LUT) function of ImageJ. (D-G) H&E-stained kidney sections of E15.5 (D,E) and newborn (NB) (F,G) α3$^{f/f}$α6$^{f/f}$ and Hoxb7cre:α3$^{f/f}$α6$^{f/f}$ kidneys are shown. There were no differences in the morphology at E15.5 (D,E), but the NB Hoxb7cre:α3$^{f/f}$α6$^{f/f}$ kidneys have fewer tubules in the inner medulla (G, indicated by arrows) compared to α3$^{f/f}$α6$^{f/f}$ mice (F), suggesting a subtle branching defect. (H-M) Newborn α3$^{f/f}$α6$^{f/f}$ and Hoxb7cre:α3$^{f/f}$α6$^{f/f}$ kidneys were immunostained with aquaporin 2 (Aqp2; magenta) and DAPI, and imaged by confocal microscopy. The black and white panels (J,K) are grayscale conversions of the Aqp2 channel using the LUT function of ImageJ, and a magnified area is shown in L and M (as indicated by the red boxed areas in J and K). (N) The number of aquaporin^{+} collecting ducts per 300 by 300 µm field were quantified. Data are presented as the mean±s.e.m. *P<0.05 between Hoxb7cre:α3$^{f/f}$α6$^{f/f}$ and α3$^{f/f}$α6$^{f/f}$ kidneys (two-tailed, unpaired t-test). Scale bars: 15 µm (B, C); 100 µm (D,E); 200 µm (F-I).

Journal of Cell Science (2021) 134, jcs259161. doi:10.1242/jcs.259161

was 234 days, whereas there was no mortality in littermate controls over the same period. To identify the etiology for the increased mortality, we euthanized the mice at 3 months of age. The Hoxb7cre:Itgα3/6$^{flox/flox}$ kidneys displayed a hypoplastic dysplastic papilla and there was marked inflammation surrounding the cortical collecting ducts (Fig. 2B-G, arrows). Under higher power, severe abnormalities of the tubular architecture, characterized by increased luminal cellularity, abnormal epithelial cell morphology, tubular obstruction and tubulointerstitial fibrosis were noted (Fig. 2H,I). As we aged the mice to over 1 year, the kidney phenotype progressed and large areas within the kidney tubulointerstitium were filled with closely packed inflammatory cells (Fig. 2J,K). The tubular cells were severely dysmorphic and appeared mesenchymal, and there was complete disorganization of the tubules (Fig. 2L,M). The mutant kidneys also displayed increased fibrosis, as verified by positive Picrosirius Red staining (Fig. 2N,O). Despite the major morphological abnormalities, there was normal expression of the laminin α3 and α5 chains in the papilla of the kidney (Fig. 2P-S). There were also no differences in laminin staining when we used a pan-laminin antibody (data not shown). Thus, the defects were not due to diminished secretion of the major laminins (111, 511, 521 and 332) found in the kidney collecting system. Taken together, these data show that although the Hoxb7cre:Itgα3/6$^{flox/flox}$ mice only had a mild ureteric bud branching defect at birth, they developed progressive tubular pathology, tubulointerstitial fibrosis and severe inflammation.

To investigate whether the collecting duct cells were more mesenchymal in the Hoxb7cre:Itgα3/6$^{flox/flox}$ mice compared to

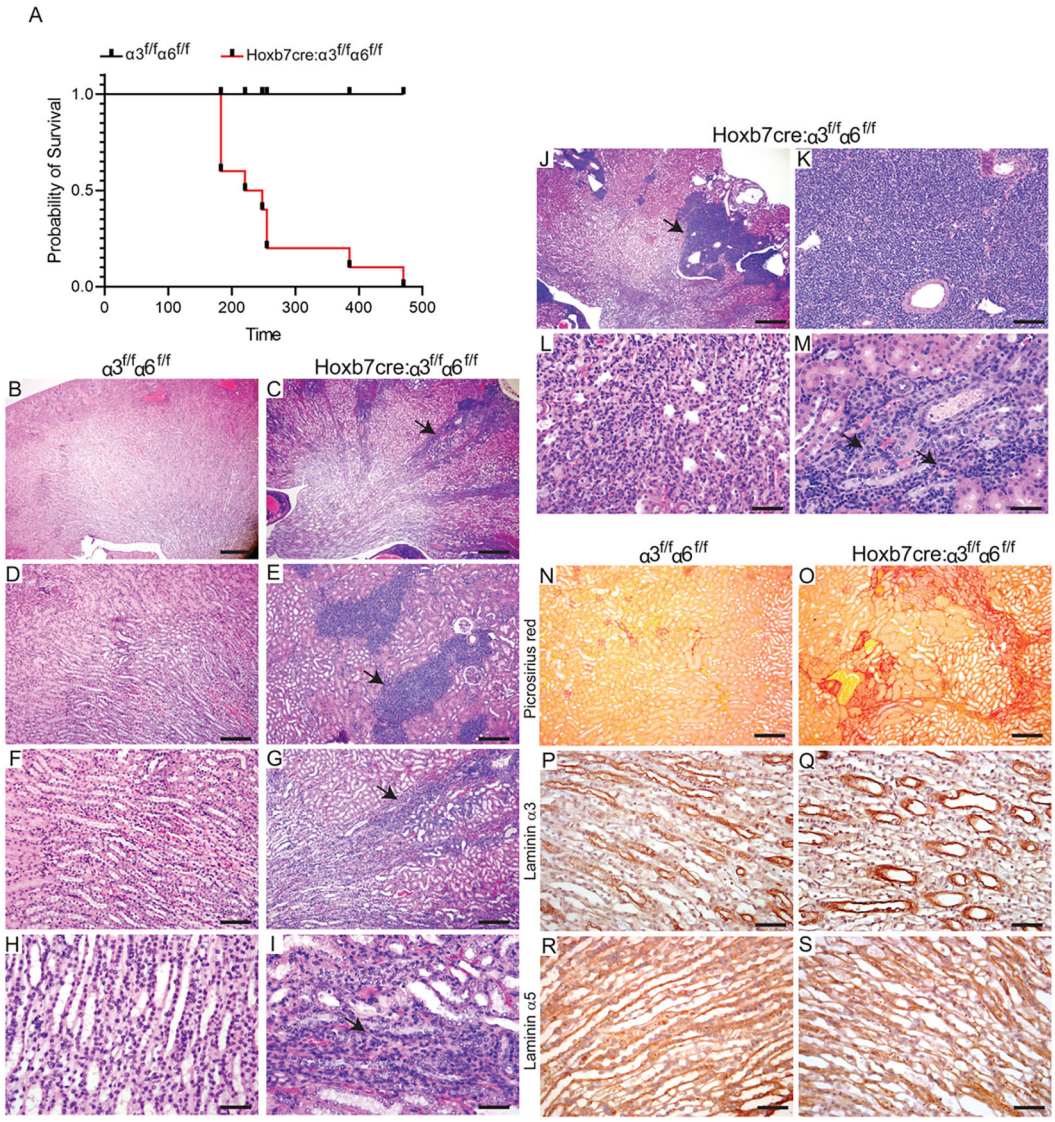

Fig. 2. Deletion of integrin α3 and α6 subunits in the ureteric bud results in inflammation and fibrosis in adult kidneys. (A) A Kaplan–Meier curve demonstrating the mortality of the Hoxb7cre:α3$^{f/f}$α6$^{f/f}$ mice over time. (B-I) H&E-stained kidneys of 4-month-old Hoxb7cre:α3$^{f/f}$α6$^{f/f}$ mice showed increased inflammatory cells surrounding the cortical collecting ducts (C,E indicated by arrows), and obstruction and dilatation of the collection ducts due to epithelial cells growing within the tubular lumens (G,I, indicated by arrows), compared with α3$^{f/f}$α6$^{f/f}$ (B,D,F,H). (J-M) H&E-stained kidney sections from 12-month-old Hoxb7cre:α3$^{f/f}$α6$^{f/f}$ mice are shown. The kidneys have large suppurative lesions (J, arrow) that are packed with leukocytes (J,K). The epithelial cells within the collecting ducts are dysmorphic and obstruct the kidney collecting ducts (L,M, arrows in M). (N,O) Picrosirius Red-stained histological sections showed increased fibrosis adjacent to dilated collecting ducts in 12-month-old Hoxb7cre:α3$^{f/f}$α6$^{f/f}$ kidneys (O) compared to α3$^{f/f}$α6$^{f/f}$ controls (N). (P-S) Six-month-old kidneys of Hoxb7cre:α3$^{f/f}$α6$^{f/f}$ and α3$^{f/f}$α6$^{f/f}$ mice were stained with antibodies against the α3 or α5 laminin chains. There were no differences in expression between the two genotypes. Scale bars: 200 µm (B,C,J); 100 µm (D-G,K,N,O); 50 µm (H,I,L,M,P-S).

Journal of Cell Science

Journal of Cell Science (2021) 134, jcs259161. doi:10.1242/jcs.259161

Itgα3/6$^{flox/flox}$ mice, we performed immunostaining of the collecting ducts and immunoblotting of the dissected pelvis of the kidney for epithelial and mesenchymal cell markers. There was a marked decrease in the expression of E-cadherin in the collecting ducts [depicted by positive staining for *Dolichos biflorus* agglutinin (DBA)] of 6-month-old Hoxb7cre:Itgα3/6$^{flox/flox}$ mice, and by 1 year there was virtually no expression in these animals. This loss of E-cadherin expression in aged mice was verified by immunoblotting (Fig. 3A,D). Consistent with the decreased E-cadherin expression there was increased expression of N-cadherin and α-smooth muscle actin (α-SMA, also known as ACTA2) in Hoxb7cre:Itgα3/6$^{flox/flox}$ mice collecting ducts, which was confirmed by immunoblotting (Fig. 3B-E). Thus, deleting the laminin-binding integrins in the kidney collecting system caused collecting duct cells to lose epithelial markers and acquire a mesenchymal phenotype.

As histological examination of aged Hoxb7cre:Itgα3/6$^{flox/flox}$ mouse kidneys suggested increased inflammation, we stained for macrophages (CD68) and lymphocytes (CD3) on kidney slides of 1-year-old mice. There were approximately five and 15 times more macrophages and lymphocytes, respectively, in the Hoxb7cre:Itgα3/6$^{flox/flox}$ mice compared to controls (Fig. 4A-F). We next examined the immune cell population in the whole kidney using flow cytometry by gating on cells that express leukocyte common antigen (CD45). We found that the CD45^{+} population accounted for 7% of the cells in the kidneys of Hoxb7cre:Itgα3/6$^{flox/flox}$ mice but for only 4.2% in the Itgα3/6$^{flox/flox}$ mice (Fig. 4G,H), suggesting there were excessive leukocytes in the Hoxb7cre:Itgα3/6$^{flox/flox}$

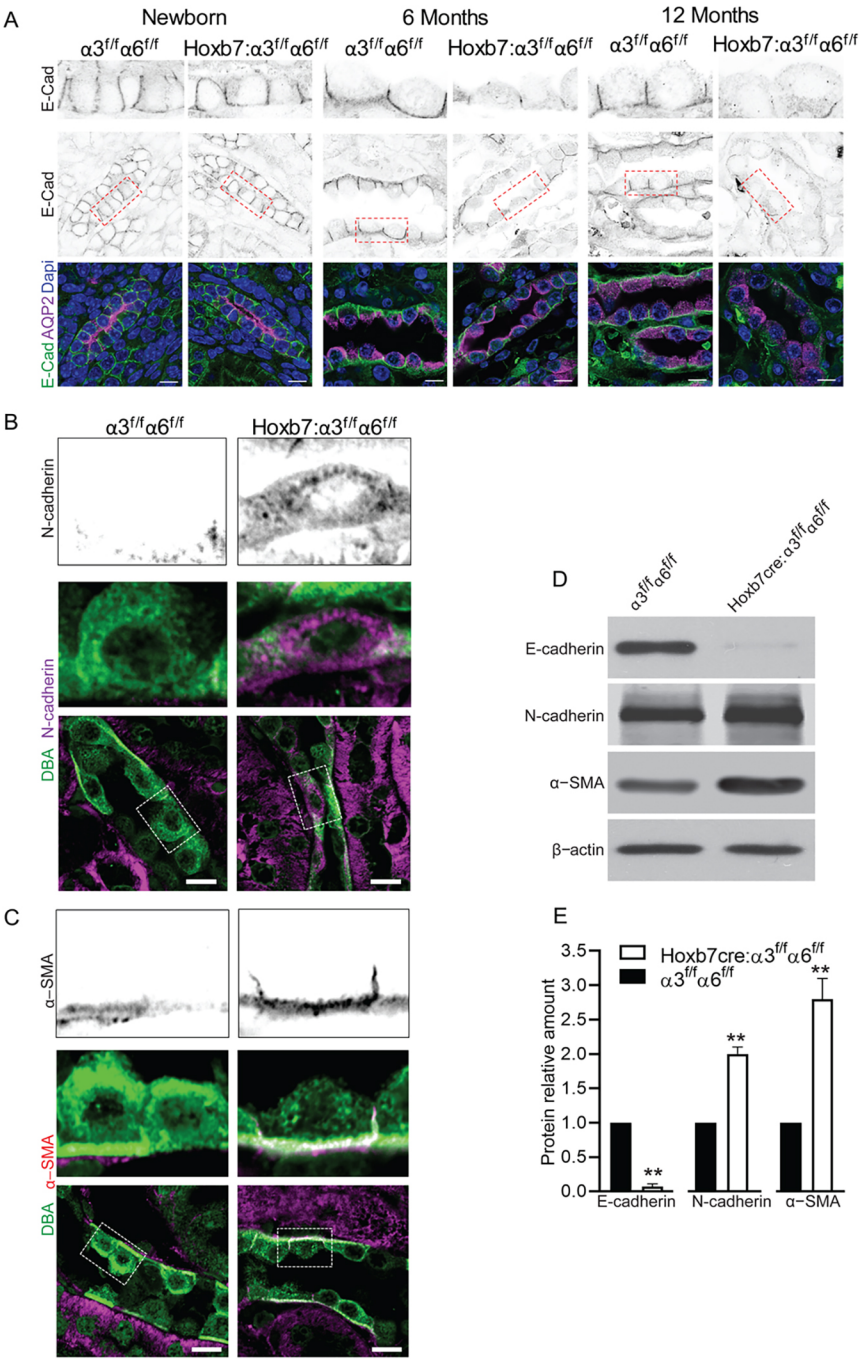

Fig. 3. Deletion of integrin α3 and α6 subunits in the ureteric bud results in loss of epithelial cell markers and acquisition of mesenchymal markers in the adult kidney collecting duct. (A) E-cadherin immune (E-cad, green) and DAPI staining (blue) were performed on newborn, 6-month-old and wild-type paraffin kidney sections, and the collecting ducts were labeled with aquaporin 2 (Aqp2, magenta). The black and white panels are grayscale conversions of the Aqp2 channel using the LUT function of ImageJ, with magnified areas highlighted by red boxes. (B,C) Collecting ducts marked by DBA (green) in Hoxb7cre:α3$^{f/f}$α6$^{f/f}$ kidney express increased mesenchymal markers N-cadherin (magenta in B) and α-SMA (magenta in C) compared to α3$^{f/f}$α6$^{f/f}$ kidneys. The black and white panels are grayscale conversions of the Aqp2 channel using the LUT function of ImageJ, with magnified areas highlighted by white boxes. (D,E) Lysates of papillae (20 µg total protein/lane) from 4-month-old α3$^{f/f}$α6$^{f/f}$ and Hoxb7cre:α3$^{f/f}$α6$^{f/f}$ mice were analyzed by western blot for levels of E-cadherin, N-cadherin and α-SMA; β-actin was used as a loading control (D). The expression of E-cadherin, N-cadherin and α-SMA was normalized to β-actin, quantified as a ratio of α3$^{f/f}$α6$^{f/f}$ kidneys, and presented as mean±s.e.m. of at least three mice (E). $^{**}P$<0.01 between Hoxb7cre:α3$^{f/f}$α6$^{f/f}$ and α3$^{f/f}$α6$^{f/f}$ samples (two-tailed, unpaired *t*-test). Scale bars: 10 µm.

Journal of Cell Science (2021) 134, jcs259161. doi:10.1242/jcs.259161

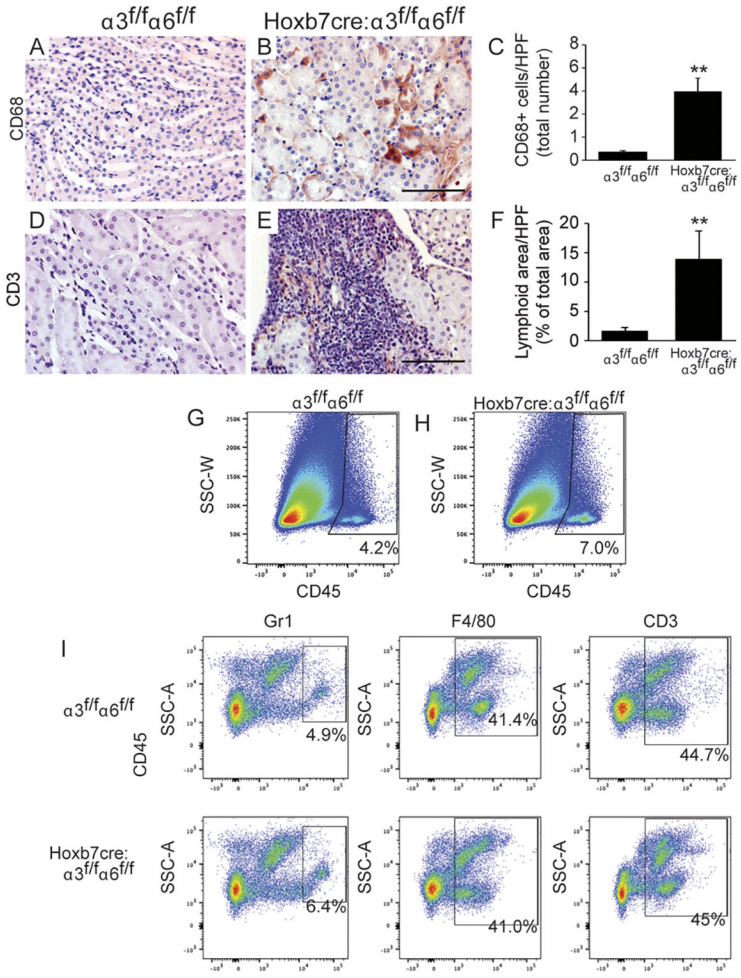

Fig. 4. Multiple inflammatory cell types are present in Hoxb7cre: $\alpha3^{f/f}\alpha6^{f/f}$ kidneys. (A-C) Immunostaining for CD68 shows areas with increased monocyte/macrophages in Hoxb7cre:$\alpha3^{f/f}\alpha6^{f/f}$ (B, brown) relative to $\alpha3^{f/f}\alpha6^{f/f}$ kidneys (A); quantified per HPF in C (n=8 of $\alpha3^{f/f}\alpha6^{f/f}$; 10 of Hoxb7cre:$\alpha3^{f/f}\alpha6^{f/f}$ mice). (D-F) Hoxb7cre:$\alpha3^{f/f}\alpha6^{f/f}$ kidneys have large areas of increased $CD3^+$ lymphoid aggregates (E, brown) relative to $\alpha3^{f/f}\alpha6^{f/f}$ kidneys (D); quantified per HPF in F (n=8 of $\alpha3^{f/f}\alpha6^{f/f}$; 10 of Hoxb7cre:$\alpha3^{f/f}\alpha6^{f/f}$ mice). (G,H) Flow cytometry on single-cell kidney suspensions demonstrates that Hoxb7cre:$\alpha3^{f/f}\alpha6^{f/f}$ mouse kidneys contain increased $CD45^+$ immune cells (n=4 mice for each $\alpha3^{f/f}\alpha6^{f/f}$ and Hoxb7cre:$\alpha3^{f/f}\alpha6^{f/f}$ group). SSC-W, side-scatter pulse width. (I) Flow cytometry demonstrates no difference in the composition of $CD45^+$ immune cell types between Hoxb7cre:$\alpha3^{f/f}\alpha6^{f/f}$ and littermate control $\alpha3^{f/f}\alpha6^{f/f}$ kidneys, with neutrophils identified by staining for Gr1, monocyte/macrophages by F4/80, and lymphocytes by CD3. SSC-A, side-scatter area. **P<0.01 between Hoxb7cre:$\alpha3^{f/f}\alpha6^{f/f}$ and $\alpha3^{f/f}\alpha6^{f/f}$ kidneys (two-tailed, unpaired t-test). Data are mean±s.e.m. of the indicated number of samples. Scale bars: 50 µm.

kidneys. When we assessed the percentages of neutrophils ($GR1^+$), macrophages ($F4/80^+$) or lymphocytes ($CD3^+$) in the $CD45^+$ leukocytes in the Hoxb7cre:Itg$\alpha3/6^{flox/flox}$ and Itg$\alpha3/6^{flox/flox}$ mice, no differences were found (Fig. 4I). Thus, there are excessive inflammatory cells within the Hoxb7cre:Itg$\alpha3/6^{flox/flox}$ kidney with no alteration in the cellular lineages.

Integrin α3/α6-null collecting duct cells acquire a mesenchymal phenotype that is leaky and allows transmigration of macrophages

To better determine how the lack of integrin α3 and α6 subunits leads to increased inflammation, we used previously generated Itg$\alpha3^{-/-}\alpha6^{-/-}$ collecting duct cells, which displayed severe deficiencies in adhesion, migration and proliferation on laminins (Yazlovitskaya et al., 2019). We initially investigated whether there was a defect in cell polarization and cell-cell tightness. Both Itg$\alpha3^{f/f}\alpha6^{f/f}$ and Itg$\alpha3^{-/-}\alpha6^{-/-}$ collecting duct cells cultured on Transwells formed monolayers. When we examined the expression levels and localization of two key components of epithelial cell-cell interaction, the expression of E-cadherin, an adherens junction component, was markedly decreased in the Itg$\alpha3^{-/-}\alpha6^{-/-}$ collecting duct cells and was primarily present in the cytoplasm rather than on the cell membrane (Fig. 5A-D,I,J). Levels of ZO-1 (also known as TJP1), a tight junction-associated protein, were significantly higher in the Itg$\alpha3^{-/-}\alpha6^{-/-}$ collecting duct cells relative to the Itg$\alpha3^{f/f}\alpha6^{f/f}$ collecting duct cells; however, like E-cadherin, this tight junction marker was not localized at the cell membrane (Fig. 5E-J). Consistent with the alterations in expression and/or localization of these epithelial markers, there was a significant increase in expression of the well-known marker of myofibroblast differentiation α-SMA, as well as N-cadherin and vimentin (Fig. 5I,J), which are more typically expressed by mesenchymal rather than polarized epithelial cells. Epithelial cells with a more mesenchymal phenotype produce profibrotic collagen I, whereas differentiated polarized epithelial cells do not (Hosper et al., 2013). Consistent with this finding, Itg$\alpha3^{-/-}\alpha6^{-/-}$ collecting duct cells express significantly more collagen I than Itg$\alpha3^{f/f}\alpha6^{f/f}$ collecting duct cells (Fig. 5I,J). Thus, deleting the α3 and α6 integrin subunits in collecting duct cells causes a major polarity defect, with the cells acquiring mesenchymal features and expressing more collagen I.

We next investigated the functional consequences of the lack of well-formed adherens junctions in the Itg$\alpha3^{-/-}\alpha6^{-/-}$ collecting duct cells in order to explain the increased inflammation observed in the Hoxb7cre:Itg$\alpha3/6^{flox/flox}$ mice. We measured the transepithelial electrical resistance (TEER) (Fig. 6A) and inulin leak, which characterize the tightness of the confluent monolayer, (Fig. 6B) in collecting duct cells grown on Transwell filters that were not coated with extracellular matrix for 96 h. TEER was significantly decreased, whereas the inulin leak was significantly increased in the Itg$\alpha3^{-/-}\alpha6^{-/-}$ collecting duct cells compared to the Itg$\alpha3^{f/f}\alpha6^{f/f}$ collecting duct cells, consistent with impaired epithelial cell-cell interactions. We next investigated the ability of a murine macrophage cell line (RAW) to transmigrate through a confluent

Journal of Cell Science (2021) 134, jcs259161. doi:10.1242/jcs.259161

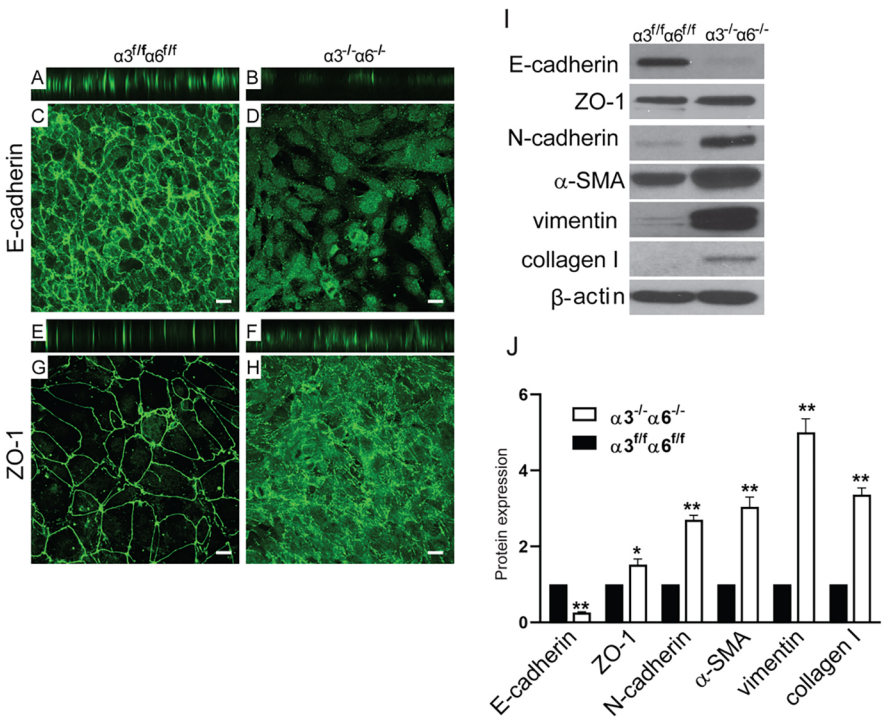

Fig. 5. $\alpha3^{-/-}\alpha6^{-/-}$ collecting duct cells have mesenchymal features and express an excessive amount of collagen I. (A-H) $\alpha3^{f/f}\alpha6^{f/f}$ and $\alpha3^{-/-}\alpha6^{-/-}$ collecting duct cells plated on Transwell filters were immunostained and imaged by confocal microscopy. (A-D) Immunostaining for E-cadherin in $\alpha3^{-/-}\alpha6^{-/-}$ collecting duct cells (B,D) showed decreased total protein expression and primarily cytoplasmic localization compared to high total protein expression and membrane localization in $\alpha3^{f/f}\alpha6^{f/f}$ collecting duct cells (A,C) as seen in both *xy* (A,B) and *z* planes (C,D). (E-H) Immunostaining shows that the polarity marker ZO-1 is not localized to the cell membranes in $\alpha3^{-/-}\alpha6^{-/-}$ collecting duct cells (F,H) relative to $\alpha3^{f/f}\alpha6^{f/f}$ collecting duct cells (E,G), in both *xy* (E,F) and *z* planes (G,H). (I,J) Total cell lysates (40 µg total protein/lane) from $\alpha3^{f/f}\alpha6^{f/f}$ and $\alpha3^{-/-}\alpha6^{-/-}$ collecting duct cells were analyzed by western blot for levels of E-cadherin, ZO-1, N-cadherin, α-SMA, vimentin and collagen I; β-actin was used as a loading control (I). The expression of proteins was normalized to β-actin, quantified as a ratio of $\alpha3^{f/f}\alpha6^{f/f}$ cells and presented as the mean±s.e.m. of at least three experiments. **P*<0.05, ***P*<0.01 between $\alpha3^{-/-}\alpha6^{-/-}$ and $\alpha3^{f/f}\alpha6^{f/f}$ collecting duct cells (two-tailed, unpaired *t*-test) (J). Scale bars: 100 µm.

monolayer of $Itg\alpha3^{f/f}\alpha6^{f/f}$ versus $Itg\alpha3^{-/-}\alpha6^{-/-}$ collecting duct cells grown on Transwell filters. Approximately 60% more RAW cells transmigrated towards regular Dulbecco's minimum Eagle medium (DMEM) when plated on top of confluent $Itg\alpha3^{-/-}\alpha6^{-/-}$ collecting duct cells compared to those on $Itg\alpha3^{f/f}\alpha6^{f/f}$ collecting duct cells (Fig. 6C). This suggests that the confluent monolayer of $Itg\alpha3^{-/-}\alpha6^{-/-}$ collecting duct cells was less tight and more permeable for macrophage transmigration.

In addition to increased permeability of the renal epithelium, another possible mechanism for the severe inflammation in the Hoxb7cre:$Itg\alpha3/6^{flox/flox}$ mouse kidney is that the collecting duct cells lacking α3 and α6 integrin subunits secrete excessive pro-inflammatory cytokines. Therefore, we placed RAW cells on top of either $Itg\alpha3^{-/-}\alpha6^{-/-}$ or $Itg\alpha3^{f/f}\alpha6^{f/f}$ collecting duct cells grown on Transwell filters and placed 24-h-conditioned medium from either $Itg\alpha3^{-/-}\alpha6^{-/-}$ or $Itg\alpha3^{f/f}\alpha6^{f/f}$ collecting duct cells in the lower chamber. The RAW cell migration was significantly higher through the $Itg\alpha3^{-/-}\alpha6^{-/-}$ collecting duct than the $Itg\alpha3^{f/f}\alpha6^{f/f}$ collecting duct cell monolayer, irrespective of the conditioned medium (Fig. 6D). Furthermore, there was significantly more migration towards the conditioned medium of the $Itg\alpha3^{-/-}\alpha6^{-/-}$ collecting duct cells in both situations. Thus, $Itg\alpha3^{-/-}\alpha6^{-/-}$ collecting duct cells have barrier function defects, and they may produce chemokines that promote RAW cell transmigration.

The laminin binding integrins regulate NF-κB activity *in vitro* and *in vivo*

The increased transmigration of the RAW cells towards the conditioned medium of $Itg\alpha3^{-/-}\alpha6^{-/-}$ collecting duct cells suggested that they secrete chemotactic factors. Therefore, we performed a multiplex analysis for chemokines on the conditioned medium of $Itg\alpha3^{f/f}\alpha6^{f/f}$ and $Itg\alpha3^{-/-}\alpha6^{-/-}$ collecting duct cells. Ten of 32 cytokines (31%), including mediators of macrophage chemotaxis, were significantly increased in the conditioned medium of $Itg\alpha3^{-/-}\alpha6^{-/-}$ collecting duct cells compared to $Itg\alpha3^{f/f}\alpha6^{f/f}$ collecting duct cells (Fig. 7A; Table S1), and many of them were recognizable gene products of NF-κB activation (including G-CSF, IL-6, KC and MIP-2). The NF-κB transcription factor complex is held in an inactive state in the cytoplasm by binding to its inhibitor IκB, which is ubiquitylated upon activation. This allows for phosphorylation of the NF-κB complex at several sites, among them serine 536 (Mattioli et al., 2004), which facilitates its shuttling into the nucleus where it can bind to promoter sites that regulate transcription of target genes (Hoffmann and Baltimore, 2006). We assessed the activity status of NF-κB in $Itg\alpha3^{-/-}\alpha6^{-/-}$ and $Itg\alpha3^{f/f}\alpha6^{f/f}$ collecting duct cells by performing immunoblotting for p65 subunit in the cytosolic and nuclear fractions, and found that the total amount (data not shown) and nuclear p65 levels were significantly higher in the $Itg\alpha3^{-/-}\alpha6^{-/-}$ collecting duct cells compared to the $Itg\alpha3^{f/f}\alpha6^{f/f}$ collecting duct cells (Fig. 7B,C). Consistent with this, there was increased serine 536 phosphorylation of p65 in the cytoplasmic fraction of $Itg\alpha3^{-/-}\alpha6^{-/-}$ collecting duct cells (Fig. 7B,D). We then verified NF-κB activity using an NF-κB luciferase reporter that contains a firefly luciferase gene under the control of a multimerized NF-κB responsive element located upstream of a minimal promoter. There was an almost twofold increase in the basal NF-κB activity in the $Itg\alpha3^{-/-}\alpha6^{-/-}$ collecting duct cells compared to the $Itg\alpha3^{f/f}\alpha6^{f/f}$ collecting duct cells. (Fig. 7E). BMS-435541 is a selective inhibitor of the IκB kinase (IKK) catalytic subunits, which inactivates NF-κB by sequestering it inactive in the cytoplasm due to masking the NF-κB nuclear localization signals. Treatment of $Itg\alpha3^{-/-}\alpha6^{-/-}$ collecting duct cells with BMS-435541 reduced NF-κB activity in these cells to the levels detected in $\alpha3^{f/f}\alpha6^{f/f}$ collecting duct cells (Fig. 7F). We also determined NF-κB activity *in vivo* by staining kidneys of 12-month-old mice with DBA, to mark the collecting ducts, and an antibody directed against serine 276 of p65 (pp65), which indicates the active form of NF-κB. Approximately 75% of collecting duct cells of Hoxb7cre:$Itg\alpha3/6^{flox/flox}$ mice had positive staining for nuclear pp65, whereas this was rarely seen in the $Itg\alpha3/6^{flox/flox}$ mice (Fig. 7G,H). Thus, deleting the laminin receptors in the collecting ducts and collecting duct cells results in significant activation of NF-κB.

Journal of Cell Science (2021) 134, jcs259161. doi:10.1242/jcs.259161

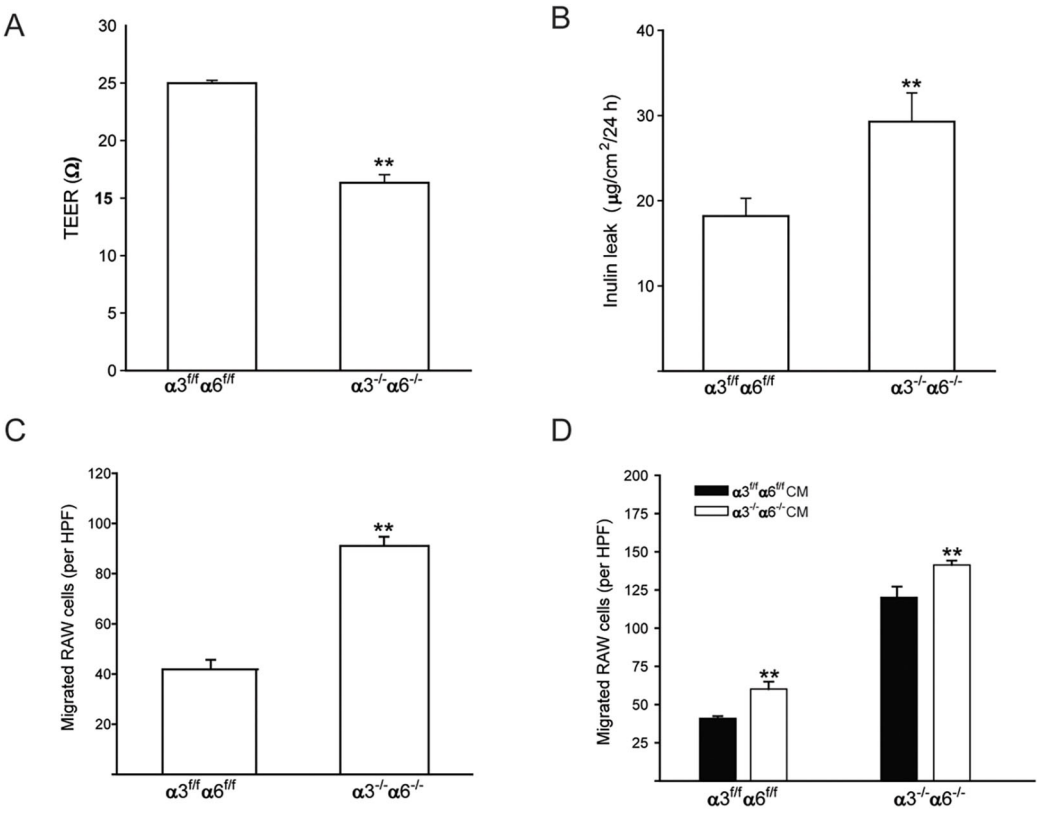

Fig. 6. $\alpha3^{-/-}\alpha6^{-/-}$ collecting duct cells have barrier function defects allowing macrophage migration. (A) $\alpha3^{-/-}\alpha6^{-/-}$ cells plated in a confluent monolayer have decreased TEER relative to $\alpha3^{f/f}\alpha6^{f/f}$ collecting duct cells. (B) Confluent monolayers of $\alpha3^{-/-}\alpha6^{-/-}$ cells permit increased leak of fluorescein-isothiocyanate-conjugated inulin across a Transwell filter compared to $\alpha3^{f/f}\alpha6^{f/f}$ cells. (C) Increased numbers of RAW macrophages migrate across a confluent monolayer of $\alpha3^{-/-}\alpha6^{-/-}$ compared to $\alpha3^{f/f}\alpha6^{f/f}$ collecting duct cells grown on a Transwell filter towards regular growth medium in the lower chamber (DMEM with 10% FBS) after 6 h of co-culture. (D) There was increased migration of RAW macrophages across a confluent monolayer of $\alpha3^{-/-}\alpha6^{-/-}$ compared to $\alpha3^{f/f}\alpha6^{f/f}$ collecting duct cells grown on Transwell filters towards 24-h conditioned medium from $\alpha3^{-/-}\alpha6^{-/-}$ compared to $\alpha3^{f/f}\alpha6^{f/f}$ collecting duct cells. Data are mean±s.e.m. of at least three experiments performed in quadruplicates (A) or triplicates (B-D). $^{**}P<0.01$ between $\alpha3^{-/-}\alpha6^{-/-}$ and $\alpha3^{f/f}\alpha6^{f/f}$ collecting duct cells (two-tailed, unpaired *t*-test).

NF-κB activity regulates the mesenchymal transition of Itg$\alpha3^{-/-}\alpha6^{-/-}$ collecting duct cells

One of the key characteristics of the Itg$\alpha3^{-/-}\alpha6^{-/-}$ collecting duct cells is that they exhibit more mesenchymal features than the Itg$\alpha3^{f/f}\alpha6^{f/f}$ collecting duct cells. The major transcription factors regulated by NF-κB that control epithelial-to-mesenchymal transitions (EMTs) are Snail and Slug (also known as Snai1 and Snai2, respectively), which accumulate in the nucleus when activated. Therefore, we investigated their activation by determining their nuclear localization (Wu et al., 2009). Immunoblots of cytosolic fractions of Itg$\alpha3^{-/-}\alpha6^{-/-}$ and Itg$\alpha3^{f/f}\alpha6^{f/f}$ collecting duct cells did not show any difference in cytosolic Snail and Slug; however, higher levels of both transcription factors were present in the nuclear fraction of Itg$\alpha3^{-/-}\alpha6^{-/-}$ collecting duct cells (Fig. 8A-C). The total levels of Snail and Slug were increased in the mutant cells (data not shown). We next defined whether downregulating the p65 subunit of NF-κB by small interfering (si)RNA affected the amount and localization of Snail or Slug in the Itg$\alpha3^{-/-}\alpha6^{-/-}$ collecting duct cells. This manipulation decreased both p65 phosphorylation at serine 536 and total p65 in the nuclear and cytosolic fractions. Consistent with the decreased expression of p65, there was a significant decrease in both Snail and Slug in the nuclear fraction of the Itg$\alpha3^{-/-}\alpha6^{-/-}$ collecting duct cells (Fig. 8D-H). These data suggest that increased NF-κB signaling in the Itg$\alpha3^{-/-}\alpha6^{-/-}$ collecting duct cells caused the mesenchymal phenotype by increasing Snail and Slug transcriptional activity.

We next determined the effects of downregulating NF-κB activity on the mesenchymal phenotype observed in the Itg$\alpha3^{-/-}\alpha6^{-/-}$ collecting duct cells by analyzing the levels of adherens junction markers, as well as collagen I. The levels of E-cadherin were increased, whereas the levels of N-cadherin were decreased in the Itg$\alpha3^{-/-}\alpha6^{-/-}$ collecting duct cells treated with p65 siRNA (Fig. 8I-M). Consistent with these results, decreased collagen I production occurred in p65 siRNA-treated Itg$\alpha3^{-/-}\alpha6^{-/-}$ collecting duct cells. These results suggest that the elevated NF-κB activity in the Itg$\alpha3^{-/-}\alpha6^{-/-}$ collecting duct cells is a major contributor to their mesenchymal phenotype and excessive collagen I production.

DISCUSSION

α3β1 and the α6 integrins functionally cooperate in cell adhesion, migration, spreading and signaling on laminin-511 and laminin-332 substrates (Yazlovitskaya et al., 2019). They are highly expressed in the developing ureteric bud and, based on *in vitro* studies, were thought to be critical for its development (Chen et al., 2004; Zent et al., 2001). However, deleting either integrin α3 or α6 subunits individually during ureteric development *in vivo* resulted in minor or no developmental phenotypes, suggesting redundancy of these integrins (Kreidberg et al., 1996; Liu et al., 2009; Viquez et al., 2017; Yazlovitskaya et al., 2015). Surprisingly, when we deleted the α3 and α6 subunits there was only a mild ureteric bud developmental phenotype that was indistinguishable from integrin α3-null mice (Kreidberg et al., 1996; Liu et al., 2009; Yazlovitskaya

Journal of Cell Science (2021) 134, jcs259161. doi:10.1242/jcs.259161

A

	G-CSF pg/ml	GM-CSF pg/ml	IL-6 pg/ml	LIF pg/ml	LIX pg/ml	KC pg/ml	MCP-1 pg/ml	MIP-1α pg/ml	MIP-2 pg/ml	RANTES pg/ml
$\alpha3^{f/f}\alpha6^{f/f}$	8.7±2.2	95.7±26.5	3.8±0.9	29.7±5.3	0.37±0.07	2002±200	3400±135	2.0±0.3	88.3±19.1	12.1±2.2
$\alpha3^{-/-}\alpha6^{-/-}$	35.0±6.7	246.9±42.1	91.9±43.5	72.5±14.4	37.8±27.2	1040± 900	6800±237	7.1±2.5	208.4±89.6	59.8±25.3
Fold-change	4.0	5.9	24.2	2.4	102.2	5.2	2.0	3.6	2.4	4.9

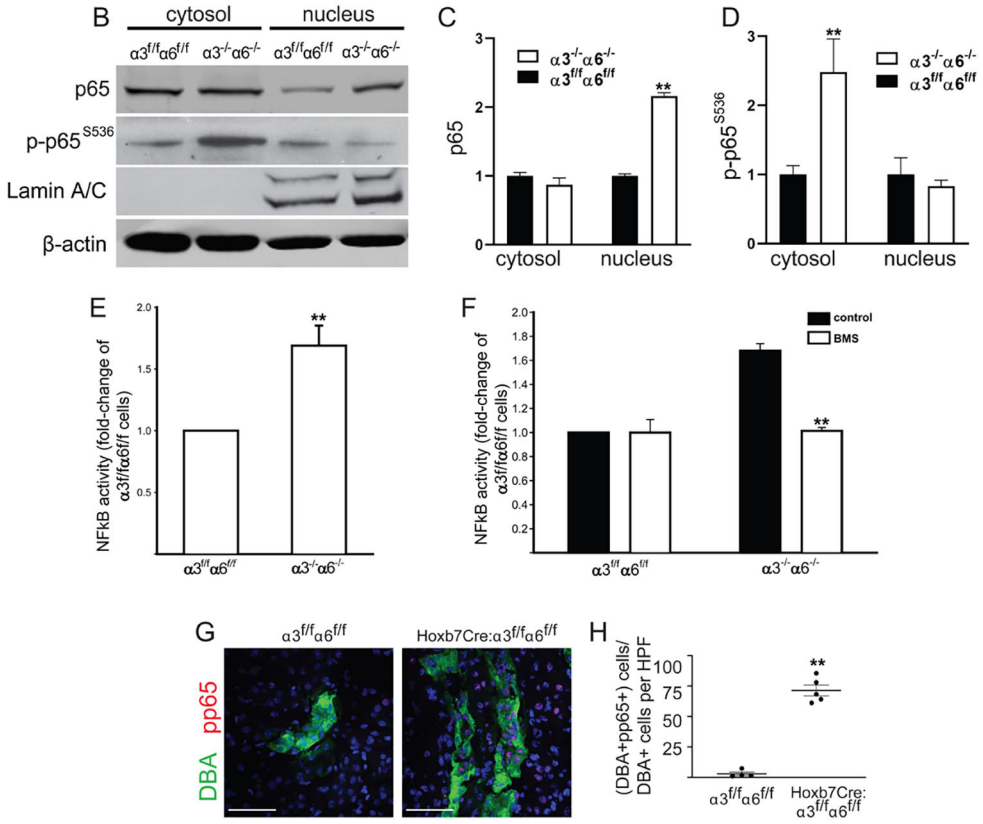

Fig. 7. $\alpha3^{-/-}\alpha6^{-/-}$ collecting duct cells exhibit increased NF-κB activation. (A) $\alpha3^{f/f}\alpha6^{f/f}$ and $\alpha3^{-/-}\alpha6^{-/-}$ collecting duct cells were grown to 80% confluence. Then, 24 h later, conditioned medium from these cells was collected and subjected to cytokine multiplex analysis. A subset of cytokines with significant differences between $\alpha3^{-/-}\alpha6^{-/-}$ and $\alpha3^{f/f}\alpha6^{f/f}$ collecting duct cells (P<0.01) are shown. (B-D) $\alpha3^{f/f}\alpha6^{f/f}$ and $\alpha3^{-/-}\alpha6^{-/-}$ collecting duct cells grown to 80% confluence were lysed and subjected to separation of nuclear and cytosolic fractions. Western blot analysis of the fractions (20 µg total protein/lane) showed increased expression of nuclear p65 and cytosolic phospho-p65^{S536} (p-p65^{S536}) in $\alpha3^{-/-}\alpha6^{-/-}$ compared to $\alpha3^{f/f}\alpha6^{f/f}$ collecting duct cells. Lamin A/C was used as a nuclear marker; β-actin was used as a loading control (B). The expression of p65 (C) or p-p65^{S536} (D) was normalized to β-actin and quantified as a ratio of $\alpha3^{f/f}\alpha6^{f/f}$ cells. (E) $\alpha3^{f/f}\alpha6^{f/f}$ and $\alpha3^{-/-}\alpha6^{-/-}$ collecting duct cells were grown to 80% confluence. Then, 24 h later, NF-kB activity in these cells was detected using a Nano-Glo Luciferase Assay and quantified as a ratio of $\alpha3^{f/f}\alpha6^{f/f}$ collecting duct cells. (F) $\alpha3^{f/f}\alpha6^{f/f}$ and $\alpha3^{-/-}\alpha6^{-/-}$ collecting duct cells grown to 80% confluence were treated with solvent (3% Tween 80 in regular growth medium) or 10 µM BMS-345541 in solvent for 1 h. NF-kB activity was detected using a Nano-Glo Luciferase Assay and quantified as a ratio of $\alpha3^{f/f}\alpha6^{f/f}$ collecting cells. (G,H) Immunostaining for the collecting duct marker DBA (green) and phospho-p65^{S276} (pp65, red) demonstrated increased NF-κB activity in both DBA$^+$ collecting duct cells and adjacent cells in Hoxb7cre:$\alpha3^{f/f}\alpha6^{f/f}$ relative to $\alpha3^{f/f}\alpha6^{f/f}$ kidneys (G). The double positive cells (DBA$^+$pp65$^+$) were quantified per HPF (H, n=5 for both genotypes of mice). Data are mean±s.e.m. of three experiments performed in triplicates. Scale bars: 50 µm. **P<0.01 between untreated and treated $\alpha3^{-/-}\alpha6^{-/-}$ collecting duct cells (F) or between Hoxb7cre:$\alpha3^{f/f}\alpha6^{f/f}$ and $\alpha3^{f/f}\alpha6^{f/f}$ kidneys (H) (two-tailed, unpaired t-test).

et al., 2015). However, these mice died at about 14 months of age due to severe inflammation, tubulointerstitial fibrosis and intratubular obstruction around the kidney collecting ducts. Mechanistically, Itgα3/α6-null collecting duct cells acquired a mesenchymal phenotype and produced excessive collagen and inflammatory cytokines, which was mediated by excessive NF-κB transcription factor pathway activation. Thus, although the laminin-binding integrins play a minor role in ureteric bud development, they are required to maintain epithelial cell polarity and downregulate epithelial cell inflammation by controlling NF-κB-dependent activity in kidney collecting ducts during normal homeostasis.

It was surprising that the deletion of both the integrin α6 and α3 subunits did not worsen ureteric bud branching morphogenesis relative to the deletion of the integrin α3 subunit only. This contradicts *in vitro* studies that show the additive effects of blocking these integrins in collecting duct epithelial cell adhesion, migration, tubulogenesis and ureteric bud development in organ culture (Chen

Journal of Cell Science (2021) 134, jcs259161. doi:10.1242/jcs.259161

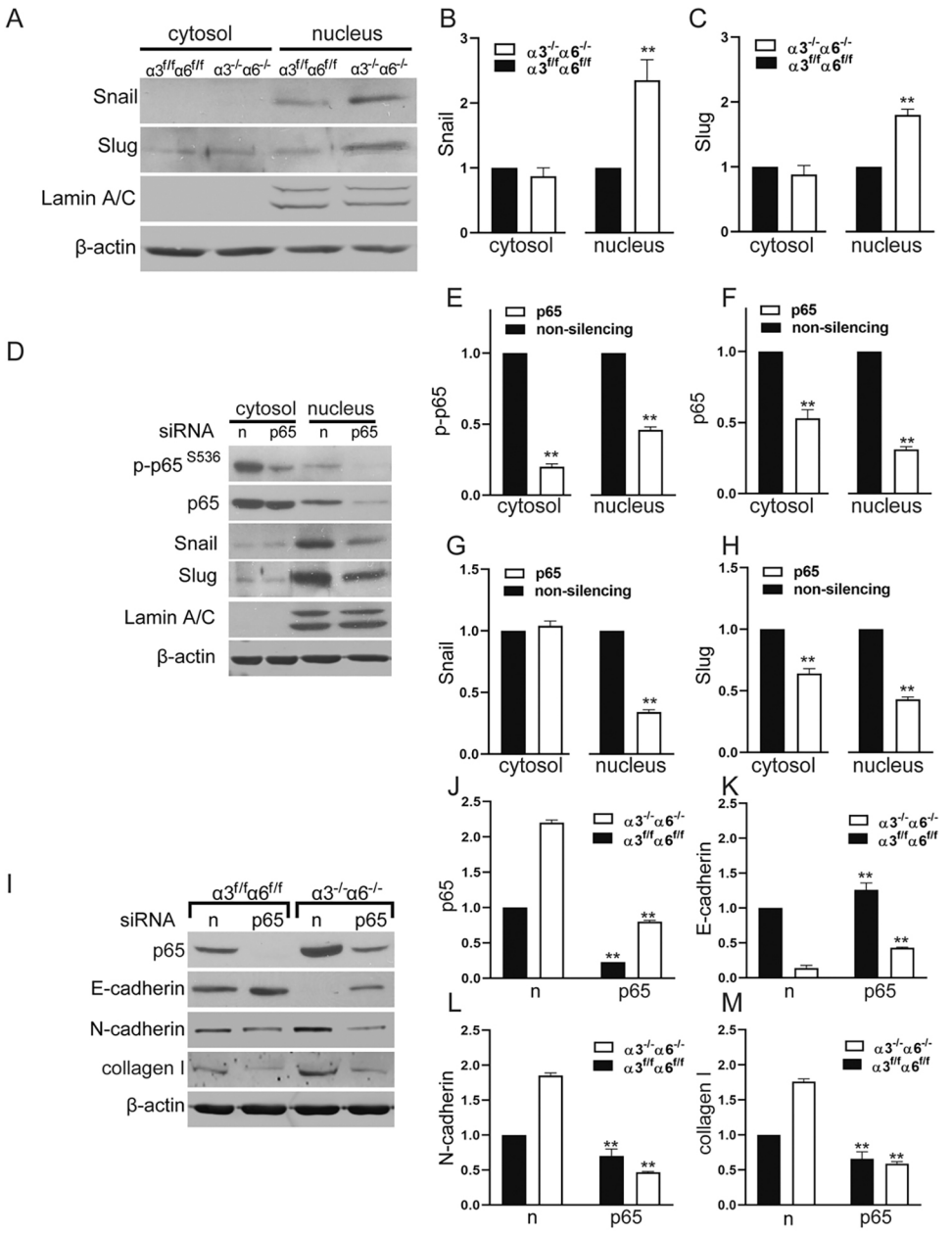

Fig. 8. The mesenchymal phenotype of $\alpha3^{-/-}\alpha6^{-/-}$ collecting duct cells is mediated by NF-κB-dependent Snail and Slug induction. (A-C) $\alpha3^{f/f}\alpha6^{f/f}$ and $\alpha3^{-/-}\alpha6^{-/-}$ collecting duct cells grown to 80% confluence were lysed and subjected to separation of nuclear and cytosolic fractions. Western blot analysis of the fractions (20 µg total protein/lane) showed increased nuclear Snail and Slug in $\alpha3^{-/-}\alpha6^{-/-}$ collecting duct cells compared to $\alpha3^{f/f}/\alpha6^{f/f}$ collecting duct cells. Lamin A/C was used as a nuclear marker; β-actin was used as a loading control (A). The expression of Snail (B) or Slug (C) was normalized to β-actin and quantified as a ratio of $\alpha3^{f/f}\alpha6^{f/f}$ cells. $^{**}P<0.01$ between $\alpha3^{-/-}\alpha6^{-/-}$ and $\alpha3^{f/f}\alpha6^{f/f}$ collecting duct cells. (D-H) $\alpha3^{-/-}\alpha6^{-/-}$ collecting duct cells grown to 80% confluence were transfected with non-silencing (n) or NF-κB p65-silencing (p65) siRNA for 48 h. Collecting duct cells were lysed and subjected to separation of nuclear and cytosolic fractions. Western blot analysis of the fractions (20 µg total protein/lane) showed decreased cytosolic and nuclear phospho-p65^{S536} (p-p65), total p65 and Slug, and decreased nuclear Snail in cells transfected with p65 siRNA compared to non-silencing siRNA. Lamin A/C was used as a nuclear marker; β-actin was used as a loading control (D). The expression of p-p65 (E), p65 (F), Snail (G) or Slug (H) was normalized to β-actin and quantified as a ratio of cells transfected with non-silencing siRNA. $^{**}P<0.01$ between cells transfected with non-silencing and p65 siRNA. (I-M) $\alpha3^{f/f}/\alpha6^{f/f}$ and $\alpha3^{-/-}\alpha6^{-/-}$ collecting duct cells grown to 80% confluence were transfected with non-silencing or NF-κB p65-silencing (p65) siRNA, and lysed 48 h later. Total cell lysates (40 µg total protein/lane) were analyzed by western blotting for levels of p65, E-cadherin, N-cadherin and collagen I; β-actin was used as a loading control (I). The expression of p65 (J), E-cadherin (K), N-cadherin (L) or collagen I (M) proteins was normalized to actin and quantified as ratio of $\alpha3^{f/f}\alpha6^{f/f}$ cells transfected with non-silencing siRNA. Data are mean±s.e.m. of at least three experiments. $^{**}P<0.01$ between non-silencing and p65 siRNA-transfected $\alpha3^{f/f}/\alpha6^{f/f}$ or $\alpha3^{-/-}/\alpha6^{-/-}$ collecting duct cells. Statistical significance was determined using two-tailed, unpaired *t*-tests.

et al., 2004; Zent et al., 2001). However, these data are consistent with observations in the global integrin α3/α6-null mouse in which the developing ureteric buds were almost normal at E16.5 when the mice died, despite having partial or complete absence of the ureters (De Arcangelis et al., 1999). The ureteric bud branching phenotype resulting from α3/α6 deletion was far less severe than the branching defect found in mice with ureteric bud deletion of the β1 integrin subunit using the same Hoxb7 cre mouse, which deletes

Journal of Cell Science (2021) 134, jcs259161. doi:10.1242/jcs.259161

β1-containing integrins that bind collagens, RGD-containing ligands and laminins (Zhang et al., 2009). Thus, in the context of the whole animal, the laminin-binding integrins play a minor role in ureteric bud development, which leaves open the question as to which integrin-ECM interactions are required for ureteric bud development. It is not integrin-collagen interactions as the integrin α1- and α2-null mice are normal (Mathew et al., 2012), and to the best of our knowledge there are no studies demonstrating a role for the RGD-binding integrins (α5β1 and αv containing integrins) in ureteric bud branching morphogenesis *in vivo*. Thus, deletion of more than one class of ligand-binding integrin is likely required to induce a major ureteric bud branching morphogenesis defect.

Despite the minimal ureteric bud branching morphogenesis defect, the Itgα3$^{-/-}$α6$^{-/-}$ collecting ducts lost many of their epithelial characteristics and acquired a mesenchymal phenotype. These changes are like those found in the developing integrin α3/α6 subunit-null mouse mammary gland in which baso-apical epithelial cell polarization is disturbed and the number of myoepithelial cells is increased (Romagnoli et al., 2020). Laminins have been shown to be the critical component of the basement membrane that enables mammary gland epithelial cells to polarize and suppress EMT via the α6-containing integrins, whereas fibronectin induces EMT via integrin α5β1 (Chen et al., 2013; Park and Schwarzbauer, 2014; Williams et al., 2008). Thus, the interaction between laminins and laminin-binding integrins appears to be critical for normal tubular epithelial cell differentiation in different branched organs.

One of our major findings in the Hoxb7cre:Itgα3/6$^{flox/flox}$ mice was the chronic inflammation with a macrophage and lymphocyte predominance around the kidney tubules that was associated with progressive fibrosis. These data are consistent with previous studies demonstrating that the deletion of the integrin α6 subunit in the gut results in colitis, which degenerates over time into infiltrating adenocarcinoma. The mechanism was that hemidesmosome disruption resulted in intestinal epithelial cells detaching from the basement membrane, which caused them to over produce IL-18, resulting in hyperplasia and enhanced intestinal permeability (De Arcangelis et al., 2017). In addition, postnatal deletion of the α6 integrin subunit in the skin resulted in chronic inflammation mediated by amphiregulin and epiregulin (Niculescu et al., 2011). A similar phenotype, characterized by chronic inflammation and emphysema, was present when the integrin β1 subunit was deleted in type 2 alveolar epithelial cells of the postnatal lung (Plosa et al., 2020). Likewise, when β1 integrin was deleted from the acinar, ductal and islet cells of the developing pancreas the mice survived but developed chronic pancreatitis with inflammatory infiltrates and mild polarity defects (Bombardelli et al., 2010). Thus, the deletion of integrins in epithelial structures that do not acquire fatal developmental phenotypes develop inflammation over time, which suggests that epithelial cell integrins play a role in suppressing this vital component of chronic injury.

We used cell culture to explore the mechanisms whereby expression of the laminin-binding integrins regulate inflammation around the collecting ducts. The Itgα3$^{-/-}$α6$^{-/-}$ collecting duct cells lost epithelial polarity, which allowed for significantly more macrophage transmigration across the monolayer. Tight and adherens junctions have been shown to be critical for leukocyte restriction in multiple organs, including the lung (Burns et al., 2003), gastrointestinal tract (Brazil et al., 2019; Ginzberg et al., 2001; Luissint et al., 2016) and uroepithelium (Parkos, 2016). There is also evidence that the transmigrating leukocytes induce disruption of barrier function (Brazil et al., 2019; Parkos, 2016). Thus, it is likely that a vicious cycle is set up in Hoxb7cre:Itgα3/6$^{flox/flox}$ mice, whereby the polarity defect increases leukocyte transmigration, which in turn causes epithelial cell injury and further increases tubule permeability. In addition to exhibiting abnormal permeability, Itgα3$^{-/-}$α6$^{-/-}$ collecting duct cells secreted high levels of inflammatory cytokines. Although this played a direct role in the increased macrophage transmigration, its effects were less profound than those mediated by the permeability defect. Increased cell permeability and excessive cytokine production was also present when the β1 integrin subunit was deleted from type 2 alveolar epithelial cells (Plosa et al., 2020).

Another key finding in our study is that loss of the integrin α3 and α6 subunits resulted in excessive NF-κB activity in the collecting duct and collecting duct cells. The role of NF-κB in kidney tubules is poorly studied and is primarily described in the setting of acute kidney injury (Henke et al., 2007; Kusch et al., 2013). In this context, downregulation of NF-κB by expressing the human NF-κB super-repressor IκBαΔN in the renal proximal tubule resulted in amelioration of injury and decreased inflammation; and targeting IKK with siRNA, which resulted in decreased NF-κB activation, attenuated renal ischemia perfusion injury in rats (Markó et al., 2016; Wan et al., 2011). These data are consistent with our finding about where excessive NF-κB activation resulted in increased injury, inflammation and secretion of inflammatory cytokines. We also showed that the mesenchymal phenotype of the Itgα3$^{-/-}$α6$^{-/-}$ collecting duct cells is due to NF-κB-dependent activation of Slug and Snail, leading to aberrant expression of adherens junctions proteins E-cadherin and N-cadherin, and accumulation of collagen I. NF-κB is an essential component of EMT and metastasis in cancer by inducing Snail stabilization by both transcriptional and posttranslational mechanisms that are highly conserved from fly to mammal (Huber et al., 2004; Skrzypek and Majka, 2020; Wu et al., 2009). The Snail genes in the kidney are highly regulated and their expression is decreased in different developmental stages so that essential epithelialization can occur (Grande et al., 2015). In addition, Snail genes are kept silent in the mature kidney as its aberrant activation is sufficient for the development of renal fibrosis (Grande et al., 2015). Thus, in Hoxb7cre:Itgα3/6$^{flox/flox}$ mice, it is likely that the usually silenced Snail family of transcription factors are activated by NF-κB-dependent signaling, which causes fibrosis and EMT.

Although we show that lack of α3 and α6 integrin subunits leads to increased NF-κB activity, an outstanding question is how this activation is achieved. We speculate that it might be in part because of the loss of integrin α3β1 binding to the ubiquitin-modifying enzyme TRAF6, which plays a role in integrin α3β1-dependent Akt activation by regulating Akt K63-linked polyubiquitylation (Yazlovitskaya et al., 2015). TRAF6 is also critical for recruiting the ubiquitin-dependent kinase transforming growth factor beta-activated kinase 1 (TAK1) and its downstream kinase IKK to assemble a signaling complex that activates NF-κB (Li et al., 2005; Li and Verma, 2002; Shi and Sun, 2018). It is therefore possible that the deletion of integrin α3β1 increases the amount of TRAF6 available to assemble TAK1/IKK complexes, resulting in excess NF-κB signaling. Clearly, integrin α3β1 binding to TRAF6 is not the only mechanism in which NF-κB signaling is regulated, as the phenotype is only present when both integrin α3 and α6 subunits are deleted and not in mice deficient of only a single integrin subunit.

In conclusion, we have demonstrated that the laminin-binding integrins only play a minor role in regulating ureteric bud development *in vivo*. However, these integrins are critical for

maintaining collecting duct homeostasis because they are required for the terminal differentiation of the collecting duct cells into a tight epithelium, and they play a crucial role in downregulating inflammatory cytokine production by these cells. These functions are mediated by modulating the NF-κB signaling pathway; a previously unrecognized critical function of integrins in polarized kidney tubule epithelial cells.

MATERIALS AND METHODS

Mice

All animal experiments were approved by the Vanderbilt University Medical Center Institutional Animal Care and Use Committee. To generate mice in which the integrin α3 and α6 subunits were deleted in the developing ureteric bud, we intercrossed Itgα3$^{flox/flox}$ (Sachs et al., 2006) and Itgα6$^{flox/flox}$ (Marchetti et al., 2013). The homozygote double mutants were then crossed with a mouse that expressed Cre recombinase under the control of the Hoxb7 promoter (Hoxb7cre) (Kobayashi et al., 2005; a gift from Dr A. McMahon, University of Southern California, USA). Littermate Itgα3/α6$^{flox/flox}$ mice that lacked Cre were used as controls. All mice are on the C57Bl/6 background. We aged Hoxb7cre:Itgα3/6$^{flox/flox}$ mice and their littermate Itgα3/6$^{flox/flox}$ controls until they either died or developed criteria requiring euthanasia. The survival differences were highly significant (P<0.002) according to both the Mantel–Cox and Gehan–Breslow–Wilcoxon tests.

Histological and morphological analysis

For histological examination, paraffin kidney sections were stained with Hematoxylin and Eosin (H&E) or Picrosirius Red, using standard protocols. For immunohistochemistry stains, paraffin sections were incubated with the primary and secondary antibodies indicated below, followed by colorimetric detection by Vector Red (Vector Laboratories). Immunofluorescence staining was performed on frozen kidney sections that were fixed with 4% paraformaldehyde, permeabilized with 0.1% Triton X-100 and incubated with the antibodies described below. Images were collected by confocal microscopy (Leica TCS SPE or Zeiss LSM710, 780 or 880, objective 63×/1.4 NA Plan Apochromat oil). The following primary antibodies were used: anti-DBA (1:100; Vector Laboratories, FL-1031); anti-CD68 (1:500; Abcam, ab53444); anti-CD3 (1:500; Abcam, ab5690); anti-Gr1 (1:500; Abcam ab238132); anti-E-cadherin (1:20; Invitrogen, 13-1900); anti-phospho-p65 (S276) (1:500; Abcam, ab106129); anti-aquaporin 2 (1:50; Cell Signaling Technology, 3487); anti-β1 integrin (1:20 in Fig. 1; BD Pharmingen, 555003 Ha2/5); anti-laminin α5 (1:250; Thermo Fisher Scientific, BS1086R); and anti-laminin α3 (1:200; Thermo Fisher Scientific, PA38937). The following secondary antibodies were used at 1:250 dilution: anti-rabbit IgG Alexa Fluor 488 (Life Technologies, A21206); anti-rabbit IgG Alexa Fluor 594 (Life Technologies, A21207); anti-mouse IgG Alexa Fluor 594 (Life Technologies, A21203); and anti-rat IgG Alexa Flour 488 (Life Technologies A21208). Quantification of immunostained sections was performed on ten non-overlapping images per kidney from a total of three kidneys obtained with a 40× objective.

Western blotting analysis for kidney tissue

The kidney papillae from individual 3-day-old pups were isolated and lysed in T-PER reagent (Thermo Scientific, Waltham, MA, USA) with protease inhibitors (Sigma-Aldrich, P8340, St. Louis, MO, USA) and phosphatase inhibitor cocktails 1 and 2 (Sigma-Aldrich, P5726 and P0044, respectively), using a Polytron homogenizer. Protein extracts (20 µg) were subjected to western blot analysis and membranes were developed using the Western Lightning Chemiluminescence Plus detection system (PerkinElmer Cetus, Wellesley, MA, USA). The following primary antibodies were used: anti-α3 integrin (1:1000; R&D Systems, AF2787); anti-α6 integrin (1:1000; Cell Signaling Technology, 3750); anti-E-cadherin (1:1000; BD Transduction Labs, 61081); anti-N-cadherin (1:1000; Cell Signaling Technology, 14215); anti-α-SMA (1:4000; Cell Signaling Technology, 19245); anti-ZO-1 (1:4000; Invitrogen, 617300); anti-vimentin (1:1000; Cell Signaling Technology, 5741); anti-phospho-NFκB p65 (S536) (1:1000; Cell Signaling Technology, 3033); anti-NFκB p65 (1:1000; Cell Signaling Technology, 8242); anti-Snail (1:500; Abcam, 53519); anti-Slug (1:500; Abcam, 27568); anti-collagen I (1:1000; Millipore, AB765P); anti-Lamin A/C (1:2000; Cell Signaling Technology, 4777); and anti-β-actin (1:10,000; Proteintech, 66009).

Flow cytometry

Single-cell whole kidney suspensions were made using collagenase XI (Sigma-Aldrich, C7657, 0.7 mg/ml) and type IV DNAse (Sigma-Aldrich, D5025, 30 µg/ml) digestion, and were subsequently passed through a 40 µm filter. Briefly, cells were blocked with anti-CD32 antibody (1:50; BD Biosciences, 553142), incubated with conjugated primary antibody and analyzed using a 5-laser BD LSRII analytical flow cytometer (BD Biosciences) and FlowJo analysis software (BD). The following primary conjugated antibodies were used in flow cytometry experiments: CD45-FITC (1:50; Invitrogen, 11-0451-82); CD3-PE-Cy7 (1:50; BioLegend, 100220); CD11b-PerCP (1:50; BioLegend, 101230); F4/80-PE (1:25; Invitrogen, MF48004); and Gr1-APC (1:50; BD Biosciences, 557661).

Cell culture

Collecting duct cells were isolated from 5-6-week-old Itgα3/6$^{flox/flox}$ mice and Itgα3/6$^{-/-}$ collecting duct cells were generated as described previously (Yazlovitskaya et al., 2019). In some experiments, the collecting duct cells were treated with IκB kinase inhibitor BMS-34554 (100 µM in water/3% Tween 80) or the vehicle alone for 1 h. To silence NFκB p65, collecting duct cells were transfected with non-silencing siRNA (20 nM, transfection control) or p65-silencing siRNA [NFκB p65 siRNA (m), 29411, Santa Cruz Biotechnology] using Lipofectamine RNAiMAX according to manufacturer's instructions. Transfected cells were used 48 h later.

Western blot analysis for collecting duct cells

Total cell lysates were prepared using M-PER reagent with protease inhibitors and phosphatase inhibitor cocktails 1 and 2. The isolation of cytoplasmic and nuclear fractions was performed using NE-PER Nuclear and Cytoplasmic Extraction Reagents (Thermo Fisher Scientific, 78833) according to the manufacturer's instructions. Protein extracts (40 µg) were subjected to western blot analysis and developed using the Western Lightning Chemiluminescence Plus detection system according to the manufacturer's protocol. Densitometry was performed using ImageJ; protein levels were normalized to β-actin.

Transepithelial electrical resistance and inulin leak assays

Tight/adherens junction tightness of collecting duct cells was measured as described previously (Basuroy et al., 2003). Resistance was measured (data presented as ohms/cm^2) on confluent monolayers of collecting duct cells using an EVOM voltmeter (World Precision Instruments, Sarasota, FL, USA). Experiments were performed three times in quadruplicates.

Inulin leak was measured on monolayers of collecting duct cells grown on Transwell filters with 8 µm pores as described previously (Basuroy et al., 2003; Elias et al., 2014). After fluorescein isothiocyanate-conjugated inulin was applied to the upper chamber, medium from the upper and lower chambers was sampled at the indicated time points. Fluorescence was detected using a Fluoroscan plate reader, and inulin leak was calculated as flux/h/cm^2. Experiments were performed three times in triplicates.

Macrophage migration assay

Monolayers of Itgα3$^{f/f}$/6$^{f/f}$ or Itgα3$^{-/-}$/α6$^{-/-}$ collecting duct cells were grown on Transwell filters with 3 µm pores (upper chamber). RAW 264.7 macrophages were placed on top of the collecting duct cells monolayers and they migrated through the collecting duct cells towards the medium in the lower chamber. The medium in the lower chamber was either regular growth medium [DMEM with 10% fetal bovine serum (FBS)] or conditioned medium collected from either Itgα3$^{f/f}$/6$^{f/f}$ or Itgα3$^{-/-}$/α6$^{-/-}$ collecting duct cells grown in confluence for 24 h. Macrophages that migrated to the underside of the Transwell filter after 6 h were fixed, stained, imaged in six non-overlapping sections and quantified as the number of migrated cells per high power field (HPF).

Multiplex assay

The cytokine/chemokine Magnetic Bead 32-Multiplex Panel (Millipore, MCYTMAG-70K-PX32) assay was performed on regular collecting duct cell growth medium conditioned for 24 h in triplicate according to the manufacturer's instructions. The assay was read on the Luminex MAGPIX platform in the Vanderbilt Hormone and Analytical Services Core.

NF-κB activity luciferase reporter assay

Itgα3$^{f/f}$/6$^{f/f}$ or Itgα3$^{-/-}$/α6$^{-/-}$ collecting duct cells (50,000 cells/well) were cultured in a 96-well plate for 24 h until 90% confluence. Cells were transfected with a NanoLuc Reporter Vector with the NF-κB Response Element (pNL3.2NFκB-RE[NlucP/NFκB-RE/Hygro, Promega, N1111) using FuGENE HD transfection reagent (Promega E2311). In experiments with the NF-κB inhibitor, cells were treated with solvent (3% Tween 80 in regular growth medium) or 10 µM BMS-345541 in solvent for 1 h. NF-kB activity was detected using the Nano-Glo Luciferase Assay System (Promega, N1110) according to the manufacturer's instructions and is presented as fold change of NF-kB activity of Itgα3$^{f/f}$α6$^{f/f}$ cells.

Statistics

A two-tailed Student's *t*-test was used for comparisons between two groups with results representing mean±s.e.m. For comparisons between more than two groups, one-way ANOVA was used, with secondary analysis by Tukey's test for multiple comparisons as indicated. For both statistical analyses, $P<0.05$ was considered statistically significant. All statistical analyses were performed with the use of SigmaStat software (Systat Software, San Jose, CA, USA).

Acknowledgements

We dedicate this article to our colleague Elisabeth Georges-Labouesse.

Competing interests

The authors declare no competing or financial interests.

Author contributions

Conceptualization: E.M.Y., E.P., A.S., T.S.B., A.P., R.Z.; Methodology: E.M.Y., E.P., F.B., O.M.V., G.M., L.S.G., A.P., R.Z.; Formal analysis: A.P., R.Z.; Resources: E.M.Y., E.P., O.M.V., G.M., A.D.A., E.G.-L., R.Z.; Data curation: E.M.Y., E.P., O.M.V., L.S.G.; Writing - original draft: E.M.Y., E.P., F.B., T.S.B., A.P., R.Z.; Writing - review & editing: E.M.Y., E.P., L.S.G., A.D.A., A.S., T.S.B., A.P., R.Z.; Visualization: E.P., F.B.; Supervision: R.Z.; Project administration: R.Z.; Funding acquisition: T.S.B., A.P., R.Z.

Funding

This work was supported by the US Department of Veterans Affairs (I01 BX002196 to R.Z.; 1I01BX003425 to L.S.G.; and I01 BX002025 to A.P.); the National Institutes of Health (R01 DK069921 to R.Z.; R01 HL151016 to T.S.B.; K08HL127102 and R03HL154287 to E.P.; and R01 DK119212 to A.P.); and the Vanderbilt O'Brien Kidney Center (P30-DK-114809 to R.Z., L.S.G. and A.P.). F.B. is the recipient of an American Society of Nephrology Ben J. Lipps Research Fellowship. Deposited in PMC for release after 12 months.

Peer review history

The peer review history is available online at https://journals.biologists.com/jcs/article-lookup/doi/10.1242/jcs.259161.

References

Basuroy, S., Sheth, P., Kuppuswamy, D., Balasubramanian, S., Ray, R. M. and Rao, R. K. (2003). Expression of kinase-inactive c-Src delays oxidative stress-induced disassembly and accelerates calcium-mediated reassembly of tight junctions in the Caco-2 cell monolayer. *J. Biol. Chem.* **278**, 11916-11924. doi:10.1074/jbc.M211710200

Bombardelli, L., Carpenter, E. S., Wu, A. P., Alston, N., DelGiorno, K. E. and Crawford, H. C. (2010). Pancreas-specific ablation of beta1 integrin induces tissue degeneration by disrupting acinar cell polarity. *Gastroenterology* **138**, 2531-2540e1-4. doi:10.1053/j.gastro.2010.02.043

Brazil, J. C., Quiros, M., Nusrat, A. and Parkos, C. A. (2019). Innate immune cell-epithelial crosstalk during wound repair. *J. Clin. Invest.* **129**, 2983-2993. doi:10.1172/JCI124618

Burns, A. R., Smith, C. W. and Walker, D. C. (2003). Unique structural features that influence neutrophil emigration into the lung. *Physiol. Rev.* **83**, 309-336. doi:10.1152/physrev.00023.2002

Carroll, T. J. and Das, A. (2013). Defining the signals that constitute the nephron progenitor niche. *J. Am. Soc. Nephrol.* **24**, 873-876. doi:10.1681/ASN.2012090931

Chen, D., Roberts, R., Pohl, M., Nigam, S., Kreidberg, J., Wang, Z., Heino, J., Ivaska, J., Coffa, S., Harris, R. C. et al. (2004). Differential expression of collagen- and laminin-binding integrins mediates ureteric bud and inner medullary collecting duct cell tubulogenesis. *Am. J. Physiol. Renal. Physiol.* **287**, F602-F611. doi:10.1152/ajprenal.00015.2004

Chen, Q. K., Lee, K. A., Radisky, D. C. and Nelson, C. M. (2013). Extracellular matrix proteins regulate epithelial-mesenchymal transition in mammary epithelial cells. *Differentiation* **86**, 126-132. doi:10.1016/j.diff.2013.03.003

De Arcangelis, A., Mark, M., Kreidberg, J., Sorokin, L. and Georges-Labouesse, E. (1999). Synergistic activities of alpha3 and alpha6 integrins are required during apical ectodermal ridge formation and organogenesis in the mouse. *Development* **126**, 3957-3968. doi:10.1242/dev.126.17.3957

De Arcangelis, A., Hamade, H., Alpy, F., Normand, S., Bruyère, E., Lefebvre, O., Méchine-Neuville, A., Siebert, S., Pfister, V., Lepage, P. et al. (2017). Hemidesmosome integrity protects the colon against colitis and colorectal cancer. *Gut* **66**, 1748-1760. doi:10.1136/gutjnl-2015-310847

Delwel, G. O., de Melker, A. A., Hogervorst, F., Jaspars, L. H., Fles, D. L., Kuikman, I., Lindblom, A., Paulsson, M., Timpl, R. and Sonnenberg, A. (1994). Distinct and overlapping ligand specificities of the alpha 3A beta 1 and alpha 6A beta 1 integrins: recognition of laminin isoforms. *Mol. Biol. Cell* **5**, 203-215. doi:10.1091/mbc.5.2.203

Elias, B. C., Mathew, S., Srichai, M. B., Palamuttam, R., Bulus, N., Mernaugh, G., Singh, A. B., Sanders, C. R., Harris, R. C., Pozzi, A. et al. (2014). The integrin β1 subunit regulates paracellular permeability of kidney proximal tubule cells. *J. Biol. Chem.* **289**, 8532-8544. doi:10.1074/jbc.M113.526509

Ginzberg, H. H., Cherapanov, V., Dong, Q., Cantin, A., McCulloch, C. A. G., Shannon, P. T. and Downey, G. P. (2001). Neutrophil-mediated epithelial injury during transmigration: role of elastase. *Am. J. Physiol. Gastrointest. Liver Physiol.* **281**, G705-G717. doi:10.1152/ajpgi.2001.281.3.G705

Grande, M. T., Sánchez-Laorden, B., López-Blau, C., De Frutos, C. A., Boutet, A., Arévalo, M., Rowe, R. G., Weiss, S. J., López-Novoa, J. M. and Nieto, M. A. (2015). Snail1-induced partial epithelial-to-mesenchymal transition drives renal fibrosis in mice and can be targeted to reverse established disease. *Nat. Med.* **21**, 989-997. doi:10.1038/nm.3901

Henke, N., Schmidt-Ullrich, R., Dechend, R., Park, J.-K., Qadri, F., Wellner, M., Obst, M., Gross, V., Dietz, R., Luft, F. C. et al. (2007). Vascular endothelial cell-specific NF-kappaB suppression attenuates hypertension-induced renal damage. *Circ. Res.* **101**, 268-276. doi:10.1161/CIRCRESAHA.107.150474

Hoffmann, A. and Baltimore, D. (2006). Circuitry of nuclear factor kappaB signaling. *Immunol. Rev.* **210**, 171-186. doi:10.1111/j.0105-2896.2006.00375.x

Hosper, N. A., van den Berg, P. P., de Rond, S., Popa, E. R., Wilmer, M. J., Masereeuw, R. and Bank, R. A. (2013). Epithelial-to-mesenchymal transition in fibrosis: collagen type I expression is highly upregulated after EMT, but does not contribute to collagen deposition. *Exp. Cell Res.* **319**, 3000-3009. doi:10.1016/j.yexcr.2013.07.014

Huber, M. A., Azoitei, N., Baumann, B., Grünert, S., Sommer, A., Pehamberger, H., Kraut, N., Beug, H. and Wirth, T. (2004). NF-kappaB is essential for epithelial-mesenchymal transition and metastasis in a model of breast cancer progression. *J. Clin. Invest.* **114**, 569-581. doi:10.1172/JCI200421358

Kobayashi, A., Kwan, K.-M., Carroll, T. J., McMahon, A. P., Mendelsohn, C. L. and Behringer, R. R. (2005). Distinct and sequential tissue-specific activities of the LIM-class homeobox gene Lim1 for tubular morphogenesis during kidney development. *Development* **132**, 2809-2823. doi:10.1242/dev.01858

Kreidberg, J. A., Donovan, M. J., Goldstein, S. L., Rennke, H., Shepherd, K., Jones, R. C. and Jaenisch, R. (1996). Alpha 3 beta 1 integrin has a crucial role in kidney and lung organogenesis. *Development* **122**, 3537-3547. doi:10.1242/dev.122.11.3537

Kusch, A., Hoff, U., Bubalo, G., Zhu, Y., Fechner, M., Schmidt-Ullrich, R., Marko, L., Müller, D. N., Schmidt-Ott, K. M., Gurgen, D. et al. (2013). Novel signalling mechanisms and targets in renal ischaemia and reperfusion injury. *Acta Physiol. (Oxf.)* **208**, 25-40. doi:10.1111/apha.12089

Li, Q. and Verma, I. M. (2002). NF-kappaB regulation in the immune system. *Nat. Rev. Immunol.* **2**, 725-734. doi:10.1038/nri910

Li, Q., Lu, Q., Bottero, V., Estepa, G., Morrison, L., Mercurio, F. and Verma, I. M. (2005). Enhanced NF-kappaB activation and cellular function in macrophages lacking IkappaB kinase 1 (IKK1). *Proc. Natl. Acad. Sci. USA* **102**, 12425-12430. doi:10.1073/pnas.0505997102

Liu, Y., Chattopadhyay, N., Qin, S., Szekeres, C., Vasylyeva, T., Mahoney, Z. X., Taglienti, M., Bates, C. M., Chapman, H. A., Miner, J. H. et al. (2009). Coordinate integrin and c-Met signaling regulate Wnt gene expression during epithelial morphogenesis. *Development* **136**, 843-853. doi:10.1242/dev.027805

Luissint, A.-C., Parkos, C. A. and Nusrat, A. (2016). Inflammation and the intestinal barrier: leukocyte-epithelial cell interactions, cell junction remodeling, and mucosal repair. *Gastroenterology* **151**, 616-632. doi:10.1053/j.gastro.2016.07.008

Marchetti, G., De Arcangelis, A., Pfister, V. and Georges-Labouesse, E. (2013). alpha6 integrin subunit regulates cerebellar development. *Cell Adhes. Migr.* **7**, 325-332. doi:10.4161/cam.25140

Markó, L., Vigolo, E., Hinze, C., Park, J.-K., Roël, G., Balogh, A., Choi, M., Wübken, A., Cording, J., Blasig, I. E. et al. (2016). Tubular epithelial NF-kappaB activity regulates ischemic AKI. *J. Am. Soc. Nephrol.* **27**, 2658-2669. doi:10.1681/ASN.2015070748

Mathew, S., Chen, X., Pozzi, A. and Zent, R. (2012). Integrins in renal development. *Pediatr. Nephrol.* **27**, 891-900. doi:10.1007/s00467-011-1890-1

Mattioli, I., Sebald, A., Bucher, C., Charles, R.-P., Nakano, H., Doi, T., Kracht, M. and Schmitz, M. L. (2004). Transient and selective NF-kappa B p65 serine 536 phosphorylation induced by T cell costimulation is mediated by I kappa B kinase beta and controls the kinetics of p65 nuclear import. *J. Immunol.* **172**, 6336-6344. doi:10.4049/jimmunol.172.10.6336

Niculescu, C., Ganguli-Indra, G., Pfister, V., Dupé, V., Messaddeq, N., De Arcangelis, A. and Georges-Labouesse, E. (2011). Conditional ablation of integrin alpha-6 in mouse epidermis leads to skin fragility and inflammation. *Eur. J. Cell Biol.* **90**, 270-277. doi:10.1016/j.ejcb.2010.09.003

Niessen, C. M., Hogervorst, F., Jaspars, L. H., de Melker, A. A., Delwel, G. O., Hulsman, E. H. M., Kuikman, I. and Sonnenberg, A. (1994). The alpha 6 beta 4 integrin is a receptor for both laminin and kalinin. *Exp. Cell Res.* **211**, 360-367. doi:10.1006/excr.1994.1099

Park, J. and Schwarzbauer, J. E. (2014). Mammary epithelial cell interactions with fibronectin stimulate epithelial-mesenchymal transition. *Oncogene* **33**, 1649-1657. doi:10.1038/onc.2013.118

Parkos, C. A. (2016). Neutrophil-epithelial interactions: a double-edged sword. *Am. J. Pathol.* **186**, 1404-1416. doi:10.1016/j.ajpath.2016.02.001

Plosa, E. J., Young, L. R., Gulleman, P. M., Polosukhin, V. V., Zaynagetdinov, R., Benjamin, J. T., Im, A. M., van der Meer, R., Gleaves, L. A., Bulus, N. et al. (2014). Epithelial beta1 integrin is required for lung branching morphogenesis and alveolarization. *Development* **141**, 4751-4762. doi:10.1242/dev.117200

Plosa, E. J., Benjamin, J. T., Sucre, J. M., Gulleman, P. M., Gleaves, L. A., Han, W., Kook, S., Polosukhin, V. V., Haake, S. M., Guttentag, S. H. et al. (2020). beta1 Integrin regulates adult lung alveolar epithelial cell inflammation. *JCI Insight* **5**, e129259. doi:10.1172/jci.insight.129259

Pozzi, A. and Zent, R. (2003). Integrins: sensors of extracellular matrix and modulators of cell function. *Nephron Exp. Nephrol.* **94**, e77-e84. doi:10.1159/000072025

Pozzi, A. and Zent, R. (2011). Extracellular matrix receptors in branched organs. *Curr. Opin. Cell Biol.* **23**, 547-553. doi:10.1016/j.ceb.2011.04.003

Romagnoli, M., Bresson, L., Di-Cicco, A., Perez-Lanzon, M., Legoix, P., Baulande, S., de la Grange, P., De Arcangelis, A., Georges-Labouesse, E., Sonnenberg, A. et al. (2020). Laminin-binding integrins are essential for the maintenance of functional mammary secretory epithelium in lactation. *Development* **147**, dev181552. doi:10.1242/dev.181552

Sachs, N., Kreft, M., van den Bergh Weerman, M. A., Beynon, A. J., Peters, T. A., Weening, J. J. and Sonnenberg, A. (2006). Kidney failure in mice lacking the tetraspanin CD151. *J. Cell Biol.* **175**, 33-39. doi:10.1083/jcb.200603073

Shi, J. H. and Sun, S. C. (2018). Tumor necrosis factor receptor-associated factor regulation of nuclear factor kappaB and mitogen-activated protein kinase pathways. *Front. Immunol.* **9**, 1849. doi:10.3389/fimmu.2018.01849

Skrzypek, K. and Majka, M. (2020). Interplay among SNAIL transcription factor, microRNAs, long non-coding RNAs, and circular RNAs in the regulation of tumor growth and metastasis. *Cancers (Basel)* **12**, 209. doi:10.3390/cancers12010209

Vijayakumar, S., Erdjument-Bromage, H., Tempst, P. and Al-Awqati, Q. (2008). Role of integrins in the assembly and function of hensin in intercalated cells. *J. Am. Soc. Nephrol.* **19**, 1079-1091. doi:10.1681/ASN.2007070737

Viquez, O. M., Yazlovitskaya, E. M., Tu, T., Mernaugh, G., Secades, P., McKee, K. K., Georges-Labouesse, E., De Arcangelis, A., Quaranta, V., Yurchenco, P. et al. (2017). Integrin alpha6 maintains the structural integrity of the kidney collecting system. *Matrix Biol.* **57-58**, 244-257. doi:10.1016/j.matbio.2016.12.003

Wan, X., Fan, L., Hu, B., Yang, J., Li, X., Chen, X. and Cao, C. (2011). Small interfering RNA targeting IKKβ prevents renal ischemia-reperfusion injury in rats. *Am. J. Physiol. Renal. Physiol.* **300**, F857-F863. doi:10.1152/ajprenal.00547.2010

Williams, C. M., Engler, A. J., Slone, R. D., Galante, L. L. and Schwarzbauer, J. E. (2008). Fibronectin expression modulates mammary epithelial cell proliferation during acinar differentiation. *Cancer Res.* **68**, 3185-3192. doi:10.1158/0008-5472.CAN-07-2673

Wu, Y., Deng, J., Rychahou, P. G., Qiu, S., Evers, B. M. and Zhou, B. P. (2009). Stabilization of snail by NF-kappaB is required for inflammation-induced cell migration and invasion. *Cancer Cell* **15**, 416-428. doi:10.1016/j.ccr.2009.03.016

Yamada, M. and Sekiguchi, K. (2015). Molecular Basis of Laminin-Integrin Interactions. *Curr. Top. Membr.* **76**, 197-229. doi:10.1016/bs.ctm.2015.07.002

Yazlovitskaya, E. M., Tseng, H.-Y., Viquez, O., Tu, T., Mernaugh, G., McKee, K. K., Riggins, K., Quaranta, V., Pathak, A., Carter, B. D. et al. (2015). Integrin α3β1 regulates kidney collecting duct development via TRAF6-dependent K63-linked polyubiquitination of Akt. *Mol. Biol. Cell* **26**, 1857-1874. doi:10.1091/mbc.E14-07-1203

Yazlovitskaya, E. M., Viquez, O. M., Tu, T., De Arcangelis, A., Georges-Labouesse, E., Sonnenberg, A., Pozzi, A. and Zent, R. (2019). The laminin binding α3 and α6 integrins cooperate to promote epithelial cell adhesion and growth. *Matrix Biol.* **77**, 101-116. doi:10.1016/j.matbio.2018.08.010

Zent, R., Bush, K. T., Pohl, M. L., Quaranta, V., Koshikawa, N., Wang, Z., Kreidberg, J. A., Sakurai, H., Stuart, R. O. and Nigám, S. K. (2001). Involvement of laminin binding integrins and laminin-5 in branching morphogenesis of the ureteric bud during kidney development. *Dev. Biol.* **238**, 289-302. doi:10.1006/dbio.2001.0391

Zhang, X., Mernaugh, G., Yang, D.-H., Gewin, L., Srichai, M. B., Harris, R. C., Iturregui, J. M., Nelson, R. D., Kohan, D. E., Abrahamson, D. et al. (2009). beta1 integrin is necessary for ureteric bud branching morphogenesis and maintenance of collecting duct structural integrity. *Development* **136**, 3357-3366. doi:10.1242/dev.036269